

Si photodiodes



Photodiodes are photosensors that generate a current or voltage when the PN junction in the semiconductor is irradiated by light. The term photodiode can be broadly defined to include even solar batteries, but it usually means sensors that accurately detect changes in light level. HAMAMATSU Si (silicon) photodiodes can be classified by function and construction into Si photodiode (PN type), Si PIN photodiode, Si APD (avalanche photodiode), MPPC (multi-pixel photon counter), and PSD (position sensitive detector).

Si photodiodes provide the following features and are widely used to detect the presence or absence, intensity, and color of light, etc.

- Excellent linearity with respect to incident light
- Low noise
- Wide spectral response range
- Mechanically rugged
- Compact and lightweight
- Long life

The lineup of Si photodiodes we manufacture utilizing our own advanced semiconductor process technologies covers a broad spectral range from the near infrared to ultraviolet and even to high-energy regions, and features high-speed response, high sensitivity, and low noise. HAMAMATSU Si photodiodes are used in a wide range of applications including medical and analytical fields, scientific measurements, optical communications, and general electronic products. These photodiodes are available in various packages such as metal, ceramic, and plastic packages, as well as in surface mount types. HAMAMATSU also offers custom-designed devices to meet special needs.

■ HAMAMATSU Si photodiodes

Type	Features	Product examples
Si photodiode	These photodiodes feature high sensitivity and low noise, and they are specifically designed for precision photometry and general photometry in the visible range.	<ul style="list-style-type: none"> • For UV to near infrared range • For visible to near infrared range • For visible range • RGB color sensor • For vacuum ultraviolet (VUV) detection • For monochromatic light detection • For electron beam detection
Si PIN photodiode	Si PIN photodiodes deliver high-speed response when operated with a reverse voltage applied and are suitable for use in optical communications and optical disk pickup, etc.	<ul style="list-style-type: none"> • Cut-off frequency: 10 MHz or more • For YAG laser detection
Multi-element Si photodiode	Photodiode arrays consist of multiple elements formed in a linear arrangement in a single package. These photodiode arrays are used in a wide range of applications such as light position detection and spectrophotometry.	<ul style="list-style-type: none"> • Segmented photodiode • One-dimensional photodiode array
Si photodiode with preamp, Thermoelectrically cooled Si photodiode	Si photodiodes with preamp incorporate a photodiode and a preamplifier into the same package, so they are highly immune to external noise and allow compact circuit design. Thermoelectrically cooled types offer drastically improved S/N.	<ul style="list-style-type: none"> • For chemical analysis and measurement
Si photodiode for radiation detection	These detectors are comprised of a Si photodiode coupled to a scintillator. They are suited for X-ray baggage inspection and non-destructive inspection systems.	<ul style="list-style-type: none"> • Type with scintillator • Large area type
Si APD	These are high-speed, high-sensitivity photodiodes having an internal gain mechanism, and can measure low level signals.	<ul style="list-style-type: none"> • Near infrared type • Short wavelength type • Multi-element type
MPPC	MPPC is a new type of photon-counting device made up of multiple APD pixels operating in Geiger mode. MPPC is a compact opto-semiconductor that operates at room temperatures and provides excellent photon-counting capabilities.	<ul style="list-style-type: none"> • Large area type (array type) • Small package type • Thermoelectrically cooled type
PSD	These position sensors detect light spots on the active area by using surface resistance. Because it is not segmented, a PSD provides continuous position data with high resolution and fast response.	<ul style="list-style-type: none"> • One-dimensional PSD • Two-dimensional PSD

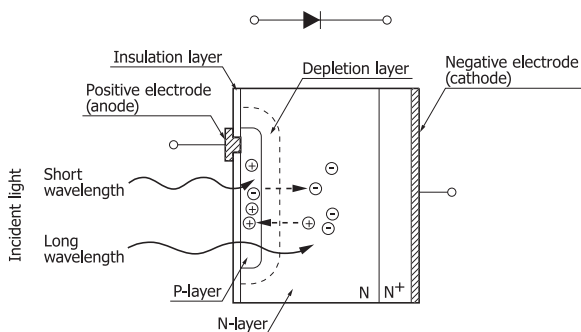
1. Si photodiodes

1-1 Principle of operation

Figure 1-1 shows a cross section example of a Si photodiode. The P-type region (P-layer) at the photosensitive surface and the N-type region (N-layer) at the substrate form a PN junction which operates as a photoelectric converter. The usual P-layer for a Si photodiode is formed by selective diffusion of boron, to a thickness of approx. 1 μm or less, and the neutral region at the junction between the P-layer and N-layer is known as the depletion layer. By controlling the thickness of the outer P-layer, N-layer, and bottom N^+ -layer as well as the dopant concentration, the spectral response and frequency response can be controlled.

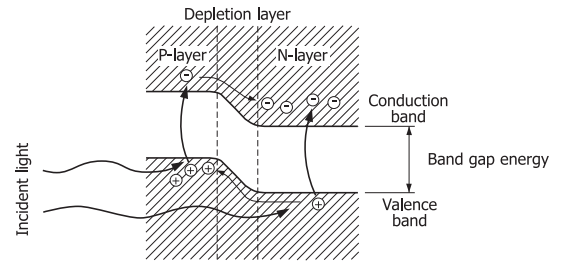
When a Si photodiode is illuminated by light and if the light energy is greater than the band gap energy, the valence band electrons are excited to the conduction band, leaving holes in their place in the valence band [Figure 1-2]. These electron-hole pairs occur throughout the P-layer, depletion layer, and N-layer materials. In the depletion layer, the electric field accelerates these electrons toward the N-layer and the holes toward the P-layer. Of the electron-hole pairs generated in the N-layer, the electrons, along with electrons that have arrived from the P-layer, are left in the N-layer conduction band. The holes at this time are being diffused through the N-layer up to the depletion layer while being accelerated, and collected in the P-layer valence band. In this manner, electron-hole pairs which are generated in proportion to the amount of incident light are collected in the N-layer and P-layer. This results in a positive charge in the P-layer and a negative charge in the N-layer. When an electrode is formed from each of the P-layer and N-layer and is connected to an external circuit, electrons will flow away from the N-layer, and holes will flow away from the P-layer toward the opposite respective electrodes, generating a current. These electrons and holes generating a current flow in a semiconductor are called the carriers.

[Figure 1-1] Schematic of Si photodiode cross section



KPDC0002EA

[Figure 1-2] Si photodiode PN junction state

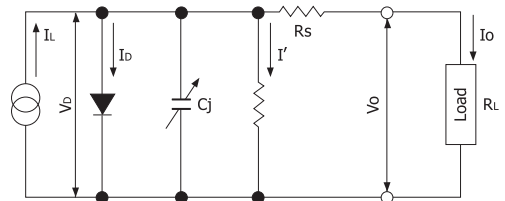


KPDC0003EA

1-2 Equivalent circuit

An equivalent circuit of a Si photodiode is shown in Figure 1-3.

[Figure 1-3] Si photodiode equivalent circuit



- I_L : current generated by incident light (proportional to light level)
- V_D : voltage across diode
- I_D : diode current
- C_j : junction capacitance
- R_{sh} : shunt resistance
- I' : shunt resistance current
- R_s : series resistance
- V_o : output voltage
- I_o : output current

KPDC0004EA

Using the above equivalent circuit, the output current (I_o) is given by equation (1).

$$I_o = I_L - I_D - I' = I_L - I_s \left(\exp \frac{q V_D}{k T} - 1 \right) - I' \dots \dots \dots (1)$$

- I_s : photodiode reverse saturation current
- q : electron charge
- k : Boltzmann's constant
- T : absolute temperature of photodiode

The open circuit voltage (V_{oc}) is the output voltage when $I_o=0$, and is expressed by equation (2).

$$V_{oc} = \frac{k T}{q} \ln \left(\frac{I_L - I'}{I_s} + 1 \right) \dots \dots \dots (2)$$

If I' is negligible, since I_s increases exponentially with respect to ambient temperature, V_{oc} is inversely proportional to the ambient temperature and proportional to the log of I_L . However, this relationship does not hold when detecting low-level light.

The short circuit current (I_{sc}) is the output current when load resistance (R_L)=0 and $V_o=0$, and is expressed by equation (3).

$$I_{sc} = I_L - I_s \left(\exp \frac{q \times I_{sc} \times R_s}{k T} - 1 \right) - \frac{I_{sc} \times R_s}{R_{sh}} \dots \dots \dots (3)$$

In equation (3), the 2nd and 3rd terms become the cause that determines the linearity limit of the short circuit current. However, since R_s is several ohms and R_{sh} is 10^7 to 10^{11} ohms, these 2nd and 3rd terms become negligible over quite a wide range.

2

1-3 Current vs. voltage characteristics

When a voltage is applied to a Si photodiode in a dark state, the current versus voltage characteristic observed is similar to the curve of a conventional rectifier diode as shown by in Figure 1-4. However, when light strikes the photodiode, the curve at shifts to and increasing the incident light level shifts this characteristic curve still further to position in parallel. As for the characteristics of and , if the photodiode terminals are shorted, a short circuit current I_{sc} or I_{sc}' proportional to the light level will flow from the anode to the cathode. If the circuit is open, an open circuit voltage V_{oc} or V_{oc}' will be generated with the positive polarity at the anode. V_{oc} changes logarithmically with changes in the light level but greatly varies with temperature, making it unsuitable for measurement of light level. Figure 1-5 shows a typical relation between I_{sc} and incident light level and also between V_{oc} and incident light level.

[Figure 1-4] Current vs. voltage characteristics

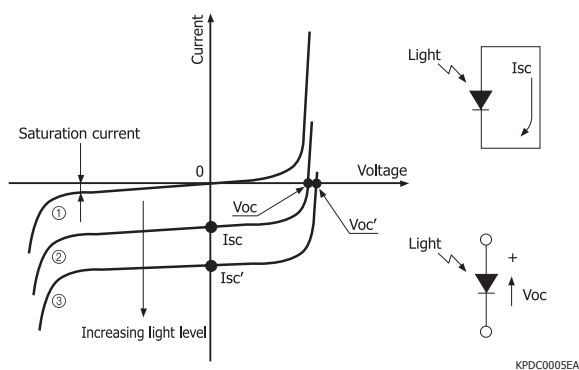
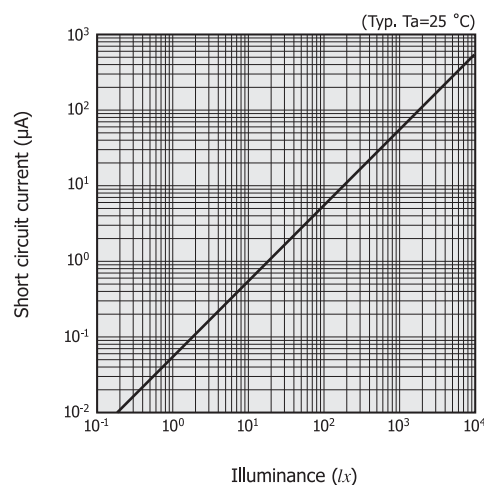


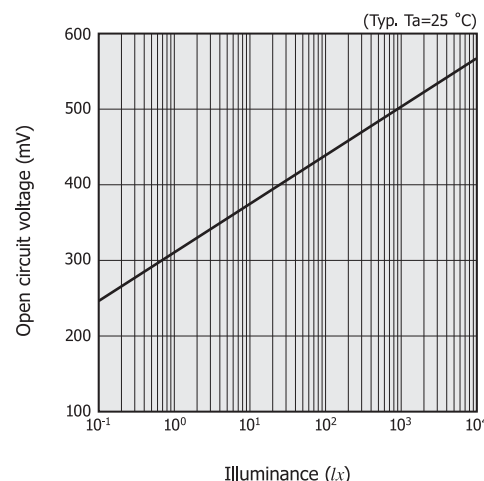
[Figure 1-5] Output signal vs. incident light level (S2386-5K)

(a) Short circuit current



KPDB0001EA

(b) Open circuit voltage

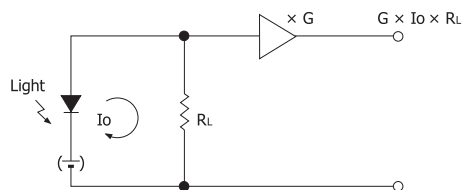


KPDB0002EA

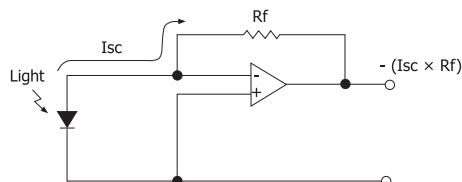
Figure 1-6 shows the basic methods of measuring a photocurrent. In the circuit shown at (a), the voltage ($I_o \times R_L$) is amplified by an amplifier with gain G . A higher linearity is maintained by applying a reverse voltage to the photodiode [Figure 1-9 (a), Figure 1-10]. The circuit shown at (b) uses an op amp to connect to the photodiode. If we let the open-loop gain of the op amp be A , the negative feedback circuit allows the equivalent input resistance (equivalent to load resistance R_L) to be R_f/A which is several orders of magnitude smaller than R_L . Thus this circuit enables ideal measurements of short circuit current. When necessary to measure the photocurrent over a wide range, the proper values of R_L and R_f must be selected to prevent output saturation even when the incident light level is high.

[Figure 1-6] Connection examples

(a) When load resistor is connected



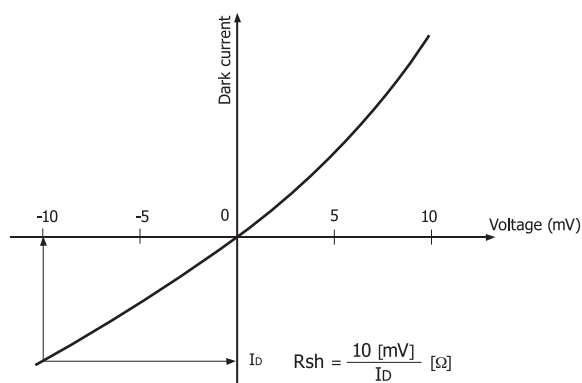
(b) When op amp is connected



KPDC0006EA

Figure 1-7 is a magnified view of the zero region of curve shown in Figure 1-4. This proves that the change in dark current (I_D) is approximately linear in a voltage range of about ± 10 mV. The slope in this straight line indicates the shunt resistance (R_{sh}), and this resistance is the cause of thermal noise current described later. For HAMAMATSU Si photodiodes, the shunt resistance values are obtained using a dark current measured with -10 mV applied.

[Figure 1-7] Dark current vs. voltage (enlarged view of zero region of curve in Figure 1-4)



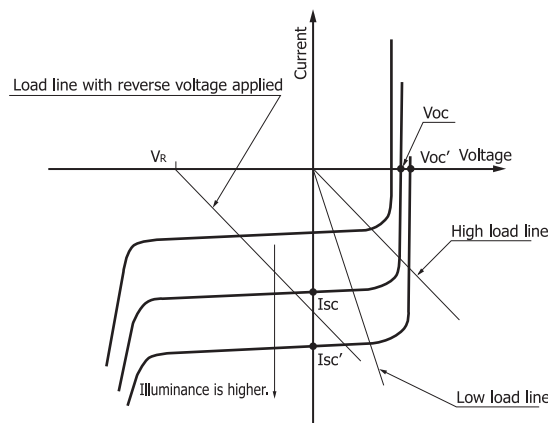
KPDB0004EA

Si photodiodes generate a power due to the photovoltaic effect, so they can operate without the need for an external power source. The photocurrent is extremely linear with respect to the incident light level. When the incident light is within the range of 10^{-12} to 10^{-2} W, the achievable range of linearity is higher than nine orders of magnitude (depending on the type of photodiode and its operating circuit, etc.). The lower limit of this linearity is determined by the noise equivalent power (NEP), while the upper limit depends on the load resistance, reverse voltage, etc., and is given by equation (4).

$$P_{sat} = \frac{V_{Bi} + V_R}{(R_S + R_L) \times S_\lambda} \dots\dots\dots (4)$$

P_{sat} : input energy [W] at upper limit of linearity ($P_{sat} \leq 10$ mW)
 V_{Bi} : contact voltage [V] (approx. 0.2 to 0.3 V)
 V_R : reverse voltage [V]
 R_L : load resistance [Ω]
 S_λ : photo sensitivity [A/W] at wavelength λ
 R_S : photodiode series resistance (several ohms)

[Figure 1-8] Current vs. voltage characteristics and load lines



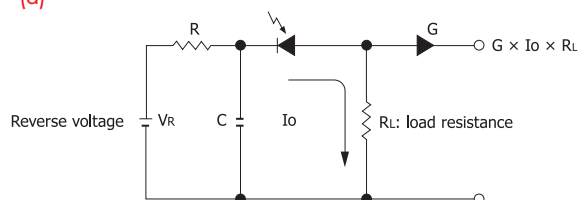
KPDB0003EC

In some cases, applying a reverse voltage is effective in enhancing the upper limit of linearity. Figure 1-9 shows connection examples for applying a reverse voltage. Figure 1-10 shows how the upper limit of linearity changes with a reverse voltage (V_R). While application of a reverse voltage to a photodiode is useful in improving the linearity, it also increases dark current and noise levels. Since an excessive reverse voltage may damage the photodiode, use a reverse voltage that will not exceed the absolute maximum rating, and make sure that the cathode is maintained at a positive potential with respect to the anode.

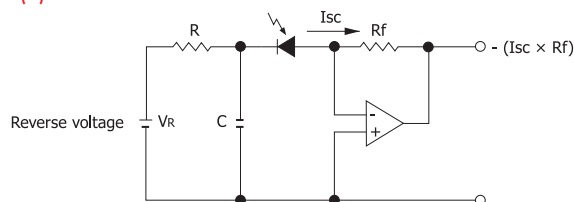
When laser light is condensed on a small spot, caution is required because the amount of light per unit area increases, and linearity deteriorates.

[Figure 1-9] Connection examples (with reverse voltage applied)

(a)



(b)



KPDC0008EC

[Figure 1-10] Output current vs. illuminance (S1223)

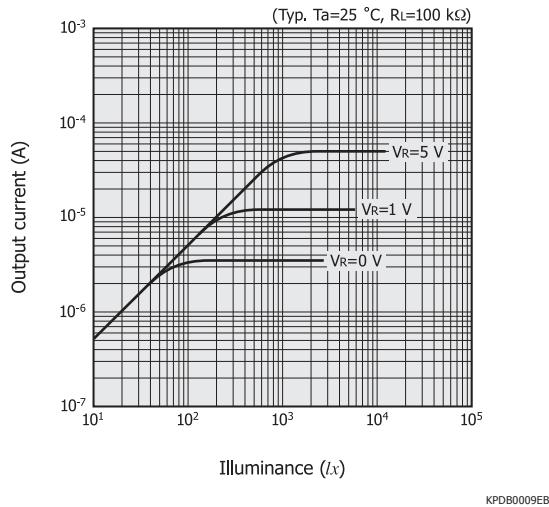
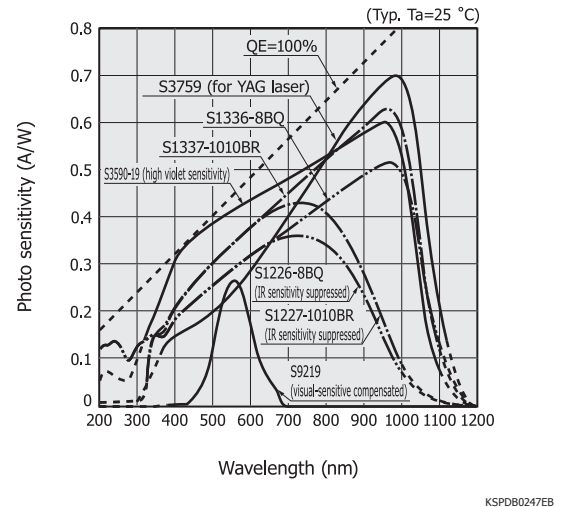


[Figure 1-11] Spectral response (Si photodiodes)



1-4 Spectral response

As explained in section 1-1, “Principle of operation,” when the energy of absorbed light is lower than the band gap energy of Si photodiodes, the photovoltaic effect does not occur. The cut-off wavelength (λ_c) can be expressed by equation (5).

$$\lambda_c = \frac{1240}{E_g} [\text{nm}] \quad \text{..... (5)}$$

Eg: band gap energy [eV]

In the case of Si at room temperature, the band gap energy is 1.12 eV, so the cut-off wavelength is 1100 nm. For short wavelengths, however, the degree of light absorption within the surface diffusion layer becomes very large [Figure 1-1]. Therefore, the thinner the diffusion layer is and the closer the PN junction is to the surface, the higher the sensitivity will be. For normal Si photodiodes, the cut-off wavelength on the short wavelength side is 320 nm, whereas it is 190 nm for UV-enhanced Si photodiodes (S1226/S1336 series, etc.).

The cut-off wavelength is determined by the intrinsic material properties of the Si photodiode, but it is also affected by the spectral transmittance of the light input window material. For borosilicate glass and plastic resin coating, wavelengths below approx. 300 nm are absorbed. If these materials are used as the window, the short-wavelength sensitivity will be lost.

When detecting wavelengths shorter than 300 nm, Si photodiodes with quartz windows are used. Measurements limited to the visible light region use a visual-sensitive compensation filter that allows only visible light to pass through it.

Figure 1-11 shows spectral responses for various types of Si photodiodes. The BQ type uses a quartz window, the BK type a borosilicate glass window, and the BR type a resin-coated window. The S9219 is a Si photodiode with a visual-sensitive compensation filter.

At a given wavelength, the number of electrons or holes that can be extracted as a photocurrent divided by the number of incident photons is called the quantum efficiency (QE). The quantum efficiency is given by equation (6).

$$QE = \frac{S \times 1240}{\lambda} \times 100 [\%] \quad \text{..... (6)}$$

S: photo sensitivity [A/W]
λ: wavelength [nm]

1-5 Noise characteristics

Like other types of photosensors, the lower limits of light detection for Si photodiodes are determined by their noise characteristics. The Si photodiode noise current (i_n) is the sum of the thermal noise current or Johnson noise current (i_j) of a resistor which approximates the shunt resistance (R_{sh}) and the shot noise currents (i_{SD} and i_{SL}) resulting from the dark current and the photocurrent.

$$i_n = \sqrt{i_j^2 + i_{SD}^2 + i_{SL}^2} [\text{A}] \quad \text{..... (7)}$$

i_j is viewed as the thermal noise of R_{sh} and is given by equation (8).

$$i_j = \sqrt{\frac{4kTB}{R_{sh}}} [\text{A}] \quad \text{..... (8)}$$

k: Boltzmann's constant
T: absolute temperature of photodiode
B: noise bandwidth

When a reverse voltage is applied as in Figure 1-9, there is always a dark current. The shot noise i_{SD} of the dark current is given by equation (9).

$$i_{SD} = \sqrt{2qI_D B} [\text{A}] \quad \text{..... (9)}$$

q: electron charge
 I_D : dark current

When a photocurrent (I_L) is generated by incident light, i_{sL} is given by equation (10).

$$i_{sL} = \sqrt{2q I_L B} \text{ [A]} \dots\dots\dots (10)$$

If $I_L \gg 0.026/R_{sh}$ or $I_L \gg I_D$, the shot noise current i_{sL} of equation (10) becomes predominant instead of the noise factor of equation (8) or (9).

The amplitudes of these noise sources are each proportional to the square root of the noise bandwidth (B) so that they are expressed in units of $A/Hz^{1/2}$ normalized by B.

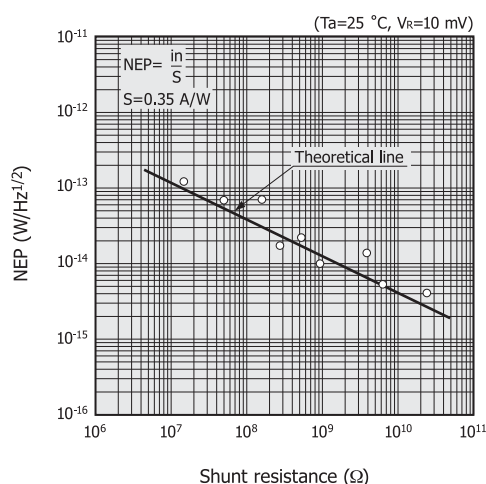
The lower limit of light detection for Si photodiodes is usually expressed as the intensity of incident light required to generate a current equal to the noise current as expressed in equation (8) or (9), which is termed the noise equivalent power (NEP).

$$NEP = \frac{i_n}{S} \text{ [W/Hz}^{1/2}] \dots\dots\dots (11)$$

i_n : noise current [$A/Hz^{1/2}$]
 S : photo sensitivity [A/W]

In cases where i_j is predominant, the relation between NEP and shunt resistance is plotted as shown in Figure 1-12. This relation agrees with the theoretical data.

[Figure 1-12] NEP vs. shunt resistance (S1226-5BK)

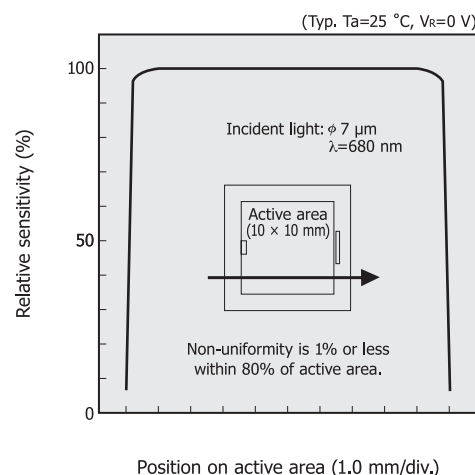


KPDB0007EA

1-6 Sensitivity uniformity

This is a measure of the sensitivity uniformity in the active area. Si photodiodes offer excellent sensitivity uniformity; their non-uniformity is usually less than 1%. This is measured with a light beam (from a laser diode, etc.) condensed to a small spot from a few microns to dozens of microns in diameter.

[Figure 1-13] Sensitivity uniformity (S1227-1010BQ)



KPDB0006EB

1-7 Response speed

The response speed of a photodiode is a measure of how fast the generated carriers are extracted to an external circuit as output current, and it is generally expressed as the rise time or cut-off frequency. The rise time is the time required for the output signal to change from 10% to 90% of the peak output value and is determined by the following factors.

- (1) Time constant t_1 of terminal capacitance C_t and load resistance R_L

C_t is the sum of the package capacitance and the photodiode junction capacitance (C_j). t_1 is given by equation (12).

$$t_1 = 2.2 \times C_t \times R_L \dots\dots\dots (12)$$

To shorten t_1 , the design must be such that C_t or R_L is made smaller. C_j is nearly proportional to the active area (A) and inversely proportional to the second to third root of the depletion layer width (d). Since the depletion layer width is proportional to the product of the reverse voltage (V_R) and the electrical resistivity (ρ) of the substrate material, equation (13) is established as follows:

$$C_j \propto A \{(V_R + 0.5) \times \rho\}^{-1/2 \text{ to } -1/3} \dots\dots\dots (13)$$

Accordingly, to shorten t_1 , a photodiode with a small A and large ρ should be used with a reverse voltage applied. However, this is advisable in cases where t_1 is a predominant factor affecting the response speed, so it should be noted that t_3 becomes slow as ρ is made large. Furthermore, applying a reverse voltage also increases dark current, so caution is necessary for use in low-light-level detection.

- (2) Diffusion time t_2 of carriers generated outside the depletion layer

Carriers may be generated outside the depletion layer

when incident light is absorbed by the area surrounding the photodiode active area and by the substrate section which is below the depletion layer. The time (t_2) required for these carriers to diffuse may sometimes be greater than several microseconds.

(3) Carrier transit time t_3 in the depletion layer

The transit speed (v_d) at which the carriers travel in the depletion layer is expressed using the carrier traveling rate (μ) and the electric field (E) in the depletion layer, as in $v_d = \mu E$. The average electric field is expressed using the reverse voltage (V_R) and depletion layer width (d), as in $E = V_R/d$, and thus t_3 can be approximated by equation (14).

$$t_3 = \frac{d}{v_d} = \frac{d^2}{\mu V_R} \dots\dots\dots (14)$$

To shorten t_3 , the distance traveled by carriers should be short or the reverse voltage higher. Since the carrier traveling rate is inversely proportional to the resistivity, t_3 becomes slower as the resistivity is increased.

The above three factors determine the rise time of a photodiode. The rise time (t_r) is approximated by equation (15).

$$t_r = \sqrt{t_1^2 + t_2^2 + t_3^2} \dots\dots\dots (15)$$

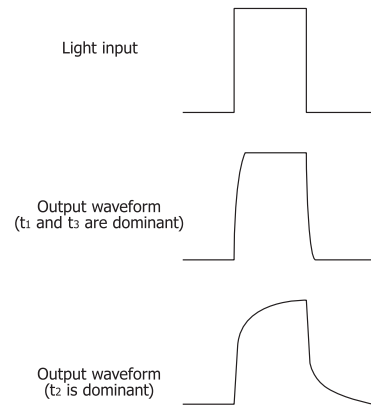
As can be seen from equation (15), the factor that is slowest among the three factors becomes predominant. As stated above, t_1 and t_3 contain the factors that contradict each other. Making one faster inevitably makes the other slower, so it is essential to create a well-balanced design that matches the application.

When a photodiode receives sine wave-modulated light emitted from a laser diode, etc., the cut-off frequency (f_c) is defined as the frequency at which the photodiode output drops by 3 dB relative to the 100% output level which is maintained while the sine wave frequency is increased. This is roughly approximated from the rise time (t_r) as in equation (16).

$$f_c = \frac{0.35}{t_r} \dots\dots\dots (16)$$

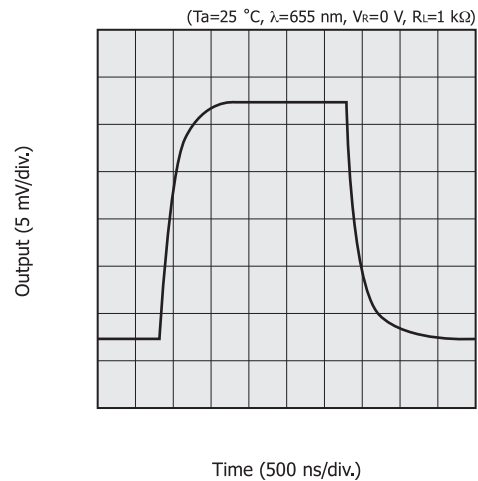
Figure 1-14 shows examples of the response waveforms and frequency characteristic for typical Si photodiodes.

[Figure 1-14] Examples of response waveforms and frequency characteristic
(a) Response waveforms



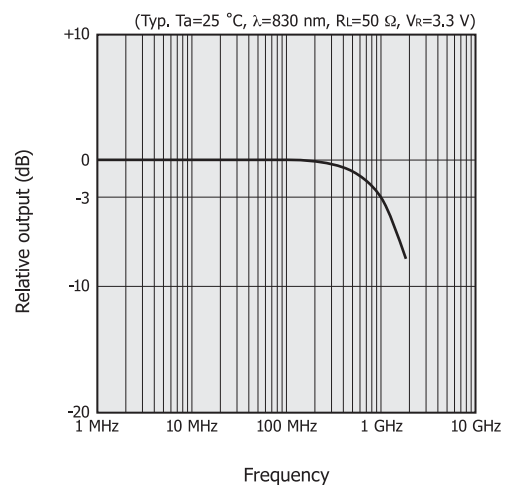
KPDC0010EB

(b) Response waveform (S2386-18K)



KPDB0010EA

(c) Frequency characteristic (S5973)



KSPDB0298EA

PIN photodiodes are designed such that fewer carriers are generated outside the depletion layer, the terminal capacitance is small, and the carrier transit time in the depletion layer is short. They are suited for optical communications and optical remote control requiring high-speed response. Even when a reverse voltage is applied, PIN photodiodes exhibit low dark

current and have excellent voltage resistance. Figure 1-15 shows changes in the cut-off frequency with increasing reverse voltage.

[Figure 1-15] Cut-off frequency vs. reverse voltage (S5973, S9055)

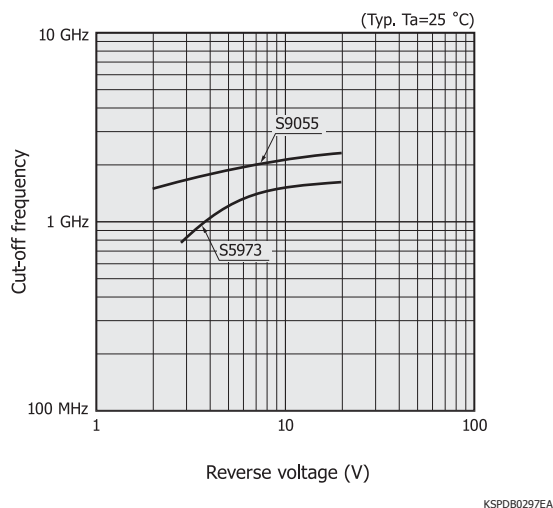
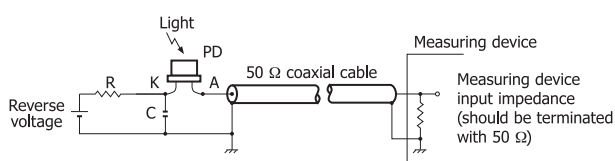


Figure 1-16 shows an example of a simple connection with 50 Ω load resistance (measurement device input impedance). The ceramic capacitor C is used to suppress oscillation which may occur from the reverse voltage power supply, while the resistor R is used to protect the Si photodiode. The resistor value is selected such that the extent of the voltage drop caused by the maximum photocurrent will be sufficiently smaller than the reverse voltage. The Si photodiode leads, capacitor leads, and coaxial cable wires carrying high-speed pulses should be kept as short as possible.

[Figure 1-16] Connection example of coaxial cable



PD: high-speed Si PIN photodiode (S5972, S5973, S9055, S9055-01, etc.)
R : 10 k Ω ; Voltage drop by photocurrent should be sufficiently lower than reverse voltage.
C : 0.1 μ F ceramic capacitor

KPDC0009EA

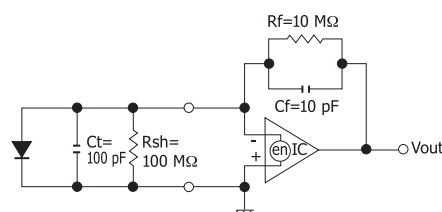
1-8 Connection to an op amp

Feedback circuit

Figure 1-17 shows a basic connection example of an op amp and Si photodiode. In the DC to low-frequency region, the voltage output V_{out} is 180 degrees out of phase with the input current (photodiode short circuit current I_{sc}) and is given by: $V_{out} = -I_{sc} \times R_f$. The feedback resistance R_f is determined by how much the input current needs to be multiplied. If, however, the feedback resistance is made greater than the photodiode shunt resistance R_{sh} , the op amp equivalent input voltage

noise (e_n) and input offset voltage will be multiplied by “1 + R_f/R_{sh} ” and then superimposed on the output voltage V_{out} . Moreover, the op amp’s bias current error (described later) will also increase, thus making it not practical to use an infinitely large feedback resistance. If there is an input capacitance C_t , the feedback capacitance C_f prevents unstable operation of the circuit in high-frequency regions. The feedback capacitance and feedback resistance also form a lowpass filter with a time constant of $C_f \times R_f$, so their values should be chosen according to the application. When it is desired to integrate the amount of incident light in applications such as radiation detection, R_f should be removed so that the op amp and C_f act as an integrating circuit. However, a switch is required to discharge C_f in order to detect continuous signals.

[Figure 1-17] Basic connection example of Si photodiode



IC: op amp
en: op amp equivalent input voltage noise

KPDC0011EA

Bias current

Since the actual input impedance of an op amp is not infinite, some bias current will flow into or out of the input terminals. This may result in error, depending on the magnitude of the detected current. The bias current which flows in an FET-input op amp is sometimes lower than 0.1 pA. Bipolar op amps, however, have bias currents ranging from several hundred picoamperes to several hundred nanoamperes. The bias current of an FET-input op amp usually increases two-fold for every increase of 10 $^{\circ}$ C in temperature, whereas that of bipolar op amp decreases with increasing temperature. In some cases, the use of a bipolar op amp should be considered when designing circuits for high-temperature operation. As is the case with offset voltage, the error voltage attributable to the bias current can be adjusted by means of a variable resistor connected to the offset adjustment terminals. Leakage currents on the printed circuit board used to configure the circuit may be greater than the op amp’s bias current. Besides selecting the optimal op amp, consideration must be given to the circuit pattern design and parts layout, as well as the use of guard rings and Teflon terminals.

Gain peaking

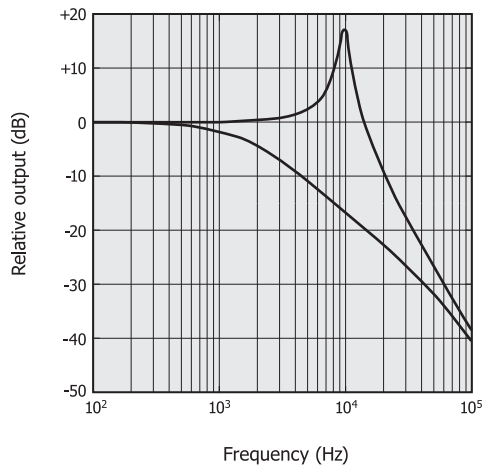
The high-frequency response characteristics of a Si photodiode and op amp circuit are determined by the time constant $R_f \times C_f$. However, if the terminal capacitance or input capacitance is

large, a phenomenon known as “gain peaking” will sometimes occur. Figure 1-18 is an example of frequency response characteristics showing gain peaking. As can be seen from the figure, the output voltage increases abnormally in the high-frequency region [see the upper trace in Figure 1-18 (a)], causing significant ringing in the output voltage waveform in response to the pulsed light input [Figure 1-18 (b)]. This gain operates in the same manner with respect to op amp input noise and may result in abnormally high noise levels [see the upper trace in Figure 1-18 (c)].

This occurs at the high-frequency region when each reactance of the input capacitance and the feedback capacitance of the op amp circuit jointly form an unstable amplifier with respect to input noise. In such a case, adverse effects on light detection accuracy may result.

[Figure 1-18] Gain peaking

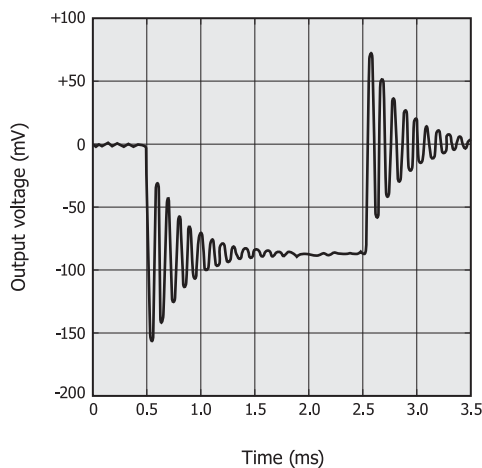
(a) Frequency characteristics



Circuit : Figure 1-17 Upper trace : Cf=0 pF
Op amp : AD549 Lower trace : Cf=10 pF
Light source : 780 nm

KPDB0019EA

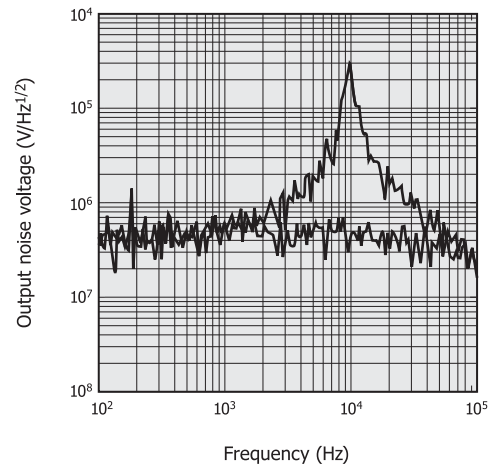
(b) Light pulse response



Circuit : Figure 1-17 Light source : 780 nm
Op amp : AD549 Cf : 0 pF

KPDB0020EA

(c) Frequency characteristics of noise output



Circuit : Figure 1-17 Upper trace : Cf=0 pF
Op amp : AD549 Lower trace : Cf=10 pF

KPDB0021EA

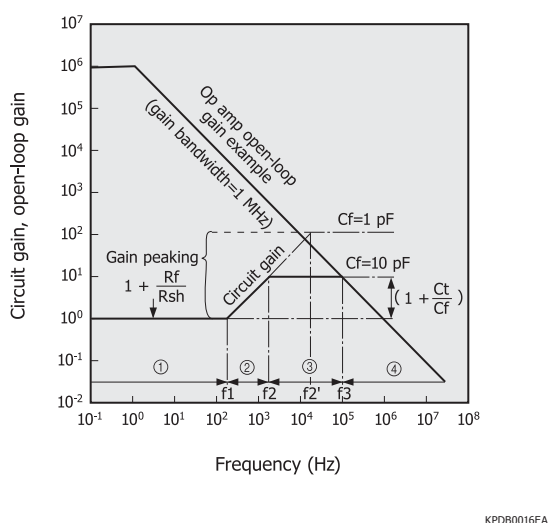
Elimination of gain peaking

To achieve a wide frequency characteristic without gain peaking and ringing phenomena, it is necessary to select the optimal relationship between the photodiode, op amp, feedback resistance, and feedback capacitance. It will prove effective in the case of photodiodes to reduce the terminal capacitance (Ct), as was previously explained in section 1-7, “Response speed.” In the op amp, the higher the speed and the wider the bandwidth, the less the gain peaking that occurs. However, if adequate internal phase compensation is not provided, oscillation may be generated as a result. Connect the feedback elements in parallel, not only the resistance but also the feedback capacitance, in order to avoid gain peaking. The gain peaking phenomena can be explained as follows, using the circuit shown in Figure 1-17.

As shown in Figure 1-19, the circuit gain of the op amp is determined for the low-frequency region simply by the resistance ratio of Rsh to Rf. From the frequency $f_1 = \frac{R_{sh} + R_f}{2\pi R_{sh} R_f (C_f + C_t)}$, gain begins to increase with frequency as shown in region . Next, at the frequency $f_2 = \frac{1}{2\pi C_f R_f}$ and above, the circuit gain of the op amp enters a flat region

which is determined by the ratio of Ct and Cf. At the point of frequency f3 where circuit gain contacts the open-loop gain line (normally, rolloff is 6 dB/octave) of the op amp, region is entered. In this example, f1 and f2 correspond to 160 Hz and 1.6 kHz, respectively, under the circuit conditions of Figure 1-17. If Cf is made 1 pF, f2 shifts to f2' and the circuit gain increases further. What should be noted here is that, since the setting of increasing circuit gain in region exceeds the open-loop gain line of the op amp, region actually does not exist. As a result, gain peaking occurs in the frequency characteristics of the op amp circuit, and ringing occurs in the pulsed light response characteristics, then instability results [Figure 1-18].

[Figure 1-19] Graphical representation of gain peaking



To eliminate gain peaking, take the following measures:

- (1) Determine R_f and C_f so that the flat region in Figure 1-19 exists.
- (2) When f_2 is positioned to the right of the open-loop gain line of the op amp, use the op amp having a high frequency at which the gain becomes 1 (unity gain bandwidth), and set region .
- (3) Replace a photodiode with a low C_t value. In the example shown in Figure 1-19, " $1 + C_t/C_f$ " should be close to 1.

The above measures (1) and (2) should reduce or prevent gain peaking and ringing. However, in the high-frequency region , circuit gain is present, and the input noise of the op amp and feedback resistance noise are not reduced, but rather, depending on the circumstances, may even be amplified and appear in the output. Measure (3) can be used to prevent this situation.

Using the above procedures, the S/N deterioration caused by gain peaking and ringing can usually be solved. However, regardless of the above measures, if load capacitance from several hundred picofarads to several nanofarads or more (for example, a coaxial cable of several meters or more and a capacitor) is connected to the op amp output, oscillation may occur in some types of op amps. Thus the load capacitance must be set as small as possible.

1-9 Application circuit examples

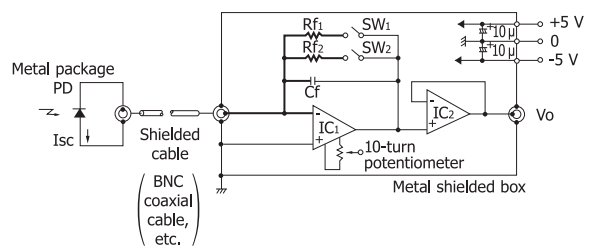
Ultra-low-light detection circuit

Ultra-low-light detection circuits require measures for reducing electromagnetic noise in the surrounding area, AC noise from the power supply, and internal op amp noise, etc.

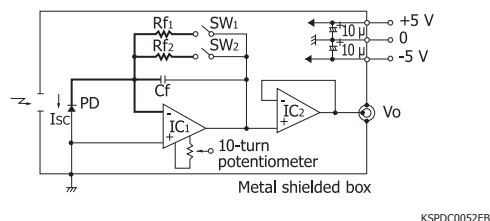
Figure 1-20 shows some measures for reducing electromagnetic noise in the surrounding area.

[Figure 1-20] Ultra-low-light sensor head

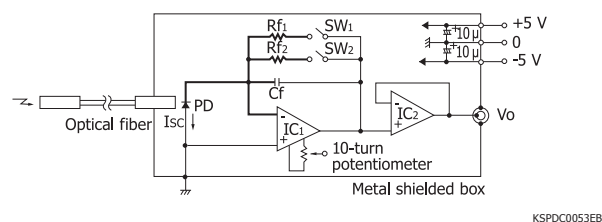
(a) Using shielded cable to connect to photodiode



(b) Using metal shielded box that contains entire circuit



(c) Using optical fiber



Bold lines should be within guarded layout or on Teflon terminals.

IC1: FET-input op amp, etc.

IC2: OP07, etc.

C_f : 10 pF to 100 pF polystyrene capacitor

R_f : 10 G Ω max.

SW: reed relay or switch with low leakage current

PD: S1226/S1336/S2386 series, S2281, etc.

$V_o = I_{sc} \times R_f [V]$

Extracting the photodiode signal from the cathode terminal is another effective means. An effective countermeasure against AC noise from the power supply is inserting an RC filter or an LC filter in the power supply line. Using a dry cell battery as the power supply also proves effective against power supply noise. Op amp noise can be reduced by selecting an op amp having a low $1/f$ noise and low equivalent input noise current. Moreover, high-frequency noise can be reduced by using a feedback capacitor (C_f) to limit the frequency bandwidth of the circuit to match the signal frequency bandwidth.

Output errors (due to the op amp input bias current and input offset voltage, routing of the circuit wiring, circuit board surface leakage current, etc.) must next be reduced. Select an FET-input op amp or a CMOS input op amp with low $1/f$ noise, both of which allow input bias currents below a few hundred femtoamperes. In addition, it will be effective to use an op amp that provides input offset voltages below several millivolts and has an offset adjustment terminal. Also use a circuit board made from materials having high insulation resistance. As countermeasures against current leakage from the surface of

the circuit board, try using a guard pattern or aerial wiring with Teflon terminals for the wiring from the photodiode to op amp input terminals and also for the feedback resistor and feedback capacitor in the input wiring.

HAMAMATSU offers the C6386-01, C9051, and C9329 photosensor amplifiers optimized for use with photodiodes for ultra-low-light detection.

[Figure 1-21] Photosensor amplifiers

(a) C6386-01

(b) C9051



(c) C9329

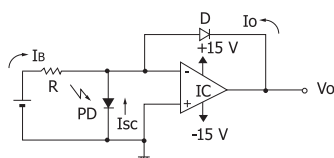


Photodiodes and coaxial cables with BNC-to-BNC plugs are sold separately.

Light-to-logarithmic voltage conversion circuit

The voltage output from a light-to-logarithmic voltage conversion circuit [Figure 1-22] is proportional to the logarithmic change in the detected light level. The log diode D for logarithmic conversion should have low dark current and low series resistance. The base-emitter (B-E) junction of a small signal transistor or the gate-source (G-S) junction of a junction FET can also be used as the log diode. I_B is the current source that supplies bias current to the log diode D and sets the circuit operating point. Unless this I_B current is supplied, the circuit will latch up when the photodiode short circuit current I_{sc} becomes zero.

[Figure 1-22] Light-to-logarithmic voltage conversion circuit



D : diode of low dark current and low series resistance
 I_B : current source for setting circuit operating point, $I_B \ll I_{sc}$
 R : 1 G Ω to 10 G Ω
 I_o : saturation current of D, 10^{-15} to 10^{-12} A
 IC: FET-input op amp

$$V_o \approx -0.06 \log \left(\frac{I_{sc} + I_B}{I_o} + 1 \right) [V]$$

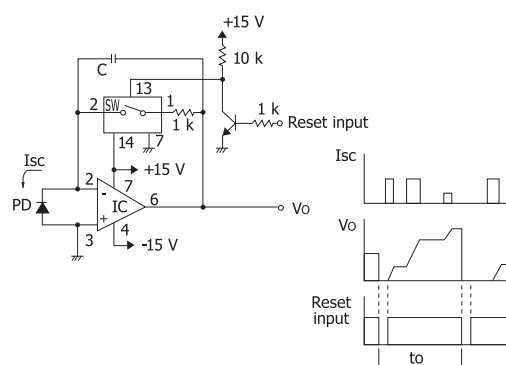
KPDC0021EA

Light quantity integration circuit

This light quantity integration circuit uses an integration

circuit made up of a photodiode and an op amp. This is used to measure the amount of integrated light or average amount of a light pulse train with irregular pulse heights, cycles, and widths. The IC in Figure 1-23 is the integrator that accumulates short circuit current I_{sc} generated by each light pulse in the integration capacitor C. By measuring the output voltage V_o immediately before reset, the average short circuit current can be obtained from the integration time ("to" in the figure) and the known value of the capacitance C. A low dielectric absorption type capacitor should be used as the capacitance C to eliminate reset errors. The switch SW is a CMOS analog switch.

[Figure 1-23] Light quantity integration circuit



Reset input: Use TTL "low" level to reset.
 IC : LF356, etc.
 SW: CMOS 4066
 PD : S1226/S1336/S2386 series, etc.
 C : polycarbonate capacitor, etc.

$$V_o = I_{sc} \times t_o \times \frac{1}{C} [V]$$

KPDC0027EB

Simple illuminometer (1)

A simple illuminometer circuit can be configured by using the HAMAMATSU C9329 photosensor amplifier and the S9219 Si photodiode with sensitivity corrected to match human eye sensitivity. As shown in Figure 1-24, this circuit can measure illuminance up to a maximum of 1000 lx by connecting the output of the C9329 to a voltmeter in the 1 V range via an external resistive voltage divider.

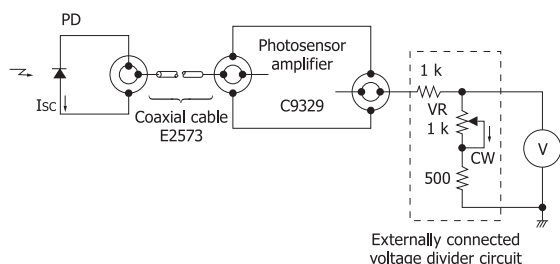
A standard light source is normally used to calibrate this circuit, but if not available, then a simple calibration can be performed with a 100 W white light source.

To calibrate this circuit, first select the L range on the C9329 and then turn the variable resistor VR clockwise until it stops. Block the light to the S9219 while in this state, and rotate the zero adjustment knob on the C9329 so that the voltmeter reads 0 mV. Next turn on the white light source, and adjust the distance between the white light source and the S9219 so that the voltmeter display shows 0.225 V. (The illuminance on the S9219 surface at this time is approx. 100 lx.) Then turn the VR counterclockwise until the voltmeter display shows 0.1 V. The calibration is now complete.

After calibration, the output should be 1 mV/lx in the L range,

and 100 mV/lx in the M range on the C9329.

[Figure 1-24] Simple illuminometer (1)



PD: S9219 (4.5 μA/100 lx)

KSPDC0054EB

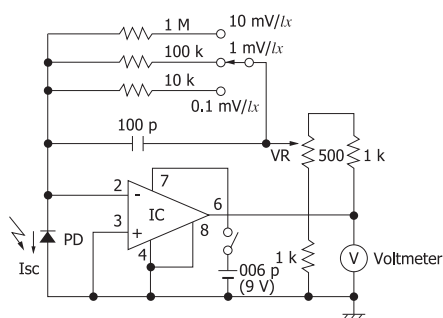
Simple illuminometer (2)

This is a simple illuminometer circuit using an op amp current-voltage conversion circuit and the S7686 Si photodiode with sensitivity corrected to match human eye sensitivity. This circuit can measure illuminance up to a maximum of 10000 lx by connecting to a voltmeter in the 1 V range.

Use a low current consumption type op amp that operates from a single power supply and allows low input bias currents. A simple calibration can be performed using a 100 W white light source.

To calibrate this circuit, first select the 10 mV/lx range and short the op amp output terminal to the sliding terminal of the variable resistor for meter calibration. Next turn on the white light source, and adjust the distance between the white light source and the S7686 so that the voltmeter reads 0.45 V. (The illuminance on the S7686 surface at this time is approx. 100 lx.) Then adjust the variable resistor for meter calibration until the voltmeter reads 1.0 V. The calibration is now complete.

[Figure 1-25] Simple illuminometer (2)



VR: variable resistor for meter calibration
IC: ICL7611, TLC271, etc.
PD: S7686 (0.45 μA/100 lx)

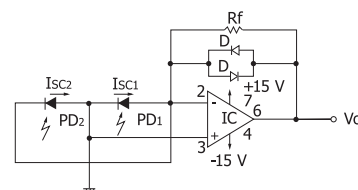
KPDC0018ED

Light balance detection circuit

Figure 1-26 shows a light balance detector circuit utilizing two Si photodiodes, PD₁ and PD₂, connected in reverse-parallel and an op amp current-voltage converter circuit. The photo sensitivity is determined by the value of the feedback resistance

R_f. The output voltage V_o becomes zero when the light levels incident on PD₁ and PD₂ are equal. Since two diodes D are connected in reverse parallel with each other, V_o will be limited to about ±0.5 V when the light levels on PD₁ and PD₂ are in an unbalanced state, so that only the light level near a balanced state can be detected with high sensitivity. If a filter is used, this circuit can also be utilized to detect a light level balance in specific wavelength regions.

[Figure 1-26] Light balance detection circuit



PD: S1226/S1336/S2386 series, etc.
IC: LF356, etc.
D: ISS270A, etc.

$V_o = R_f \times (I_{sc2} - I_{sc1})$ [V]
(Note that V_o is within ±0.5 V.)

KPDC0017EB

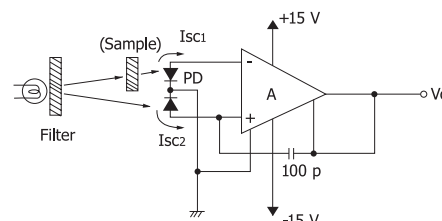
Absorptiometer

This is a light absorption meter that obtains a logarithmic ratio of two current inputs using a dedicated IC and two Si photodiodes [Figure 1-27]. By measuring the light level of the light source and the light level transmitting through a sample using two photodiodes and then comparing them, light absorbance by the sample can be measured.

To make measurements, the optical system such as an aperture diaphragm should first be adjusted so that the short circuit currents of the two photodiodes are equal and the output voltage V_o is set to 0 V. Next, the sample is placed on the light path of one photodiode. The output voltage at this point indicates the absorbance of the sample. The relation between the absorbance A and the output voltage V_o is expressed by $A = -V_o$ [V].

If necessary, a filter is placed in front of the light source as shown in Figure 1-27 in order to measure the spectral absorbance of a specific wavelength region or monochromatic light.

[Figure 1-27] Absorptiometer



A: Log amp
PD: S5870, etc.

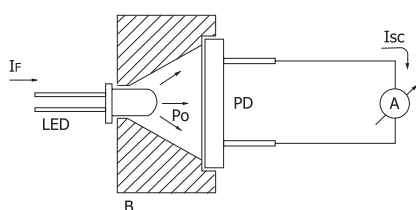
$V_o = \log (I_{sc1} / I_{sc2})$ [V]

KPDC0025EC

■ Total emission measurement of LED

Since the emitting spectral width of LED is usually as narrow as dozens of nanometers, the amount of the LED emission can be calculated from the Si photodiode photo sensitivity at a peak emission wavelength of the LED. In Figure 1-28, the inner surface of the reflector block B is mirror-processed and reflects the light emitted from the side of the LED toward the Si photodiode, so that the total amount of the LED emission can be detected by the Si photodiode [Figure 1-28].

[Figure 1-28] Total emission measurement of LED



A : ammeter, 1 mA to 10 mA
 PD: S2387-1010R
 B : aluminum block with inner surface gold-plated
 S : Si photodiode photo sensitivity
 See characteristics table in our catalog.
 S2387-1010R: $S \approx 0.58 \text{ A/W}$ at 930 nm
 P_o : total amount of emission

$$P_o \approx \frac{I_{sc}}{S} [\text{W}]$$

KPDC0026EA

■ High-speed light detection circuit (1)

This is a high-speed light detection circuit using a low-capacitance Si PIN photodiode with a reverse voltage applied and a high-speed op amp current-voltage converter circuit [Figure 1-29]. The frequency band of this circuit is limited by the op amp device characteristics to less than about 100 MHz.

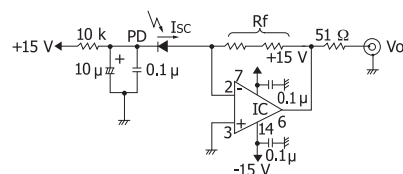
When the frequency band exceeds 1 MHz in this circuit, the lead inductance of each component and stray capacitance from feedback resistance R_f exert drastic effects on device response speed. That effect can be suppressed by using chip components to reduce the component lead inductance, and connecting multiple resistors in series to reduce stray capacitance.

The photodiode leads should be kept as short as possible, and the pattern wiring to the op amp should be made as short and thick as possible. This will lower effects from the stray capacitance and inductance occurring on the circuit board pattern of the op amp inputs and also alleviate effects from photodiode lead inductance. To enhance device performance, a ground plane structure using the entire surface of the board copper plating as the ground potential will be effective.

A ceramic capacitor should be used as the $0.1 \mu\text{F}$ capacitor connected to the op amp power line, and it should be connected to the nearest ground point in the shortest distance.

HAMAMATSU provides the C8366 photosensor amplifier for PIN photodiodes with a frequency bandwidth up to 100 MHz.

[Figure 1-29] High-speed light detection circuit (1)



PD: high-speed PIN photodiode (S5971, S5972, S5973, etc.)
 R_f : Two or more resistors are connected in series to eliminate parallel capacitance.
 IC : AD745, LT1360, HA2525, etc.

$$V_o = -I_{sc} \times R_f [\text{V}]$$

KPDC0020ED

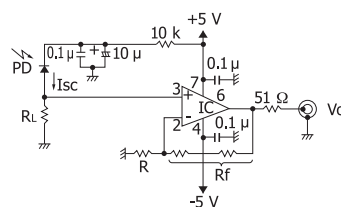
[Figure 1-30] Photosensor amplifier C8366



■ High-speed light detection circuit (2)

This high-speed light detection circuit [Figure 1-31] uses load resistance R_L to convert the short circuit current from a low-capacitance Si PIN photodiode (with a reverse voltage applied) to a voltage, and amplifies the voltage with a high-speed op amp. There is no problem with gain peaking due to phase shifts in the op amp. A circuit with a frequency bandwidth higher than 100 MHz can be fabricated by selecting the correct op amp. Points for caution in the components, pattern, and structure are the same as those listed for the “High-speed light detection circuit (1).”

[Figure 1-31] High-speed light detection circuit (2)



PD : high-speed PIN photodiode
 (S5971, S5972, S5973, S9055, S9055-01, etc.)
 R_L , R , R_f : adjusted to meet the recommended conditions of op amp
 IC : AD8001, etc.

$$V_o = I_{sc} \times R_L \times \left(1 + \frac{R_f}{R}\right) [\text{V}]$$

KPDC0015EE

■ AC light detection circuit (1)

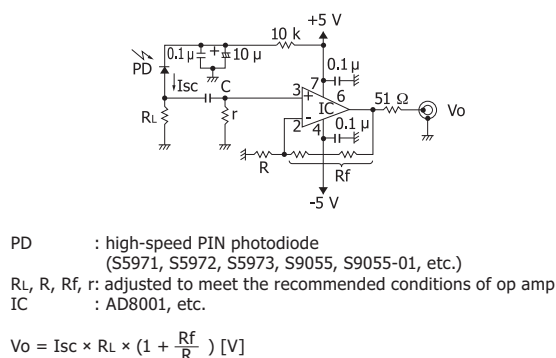
This is an AC light detection circuit [Figure 1-32] that uses load resistance R_L to convert the photocurrent from a low-capacitance Si PIN photodiode (with a reverse voltage applied) to a voltage, and amplifies the voltage with a high-speed op

amp. There is no problem with gain peaking due to phase shifts in the op amp. A circuit with a frequency bandwidth higher than 100 MHz can be fabricated by selecting the correct op amp.

Points for caution in the components, pattern, and structure are the same as those listed for the “High-speed light detection circuit (1).”

HAMAMATSU provides the C4890 amplifier for PIN photodiodes with a frequency bandwidth from 10 MHz up to 1.5 GHz.

[Figure 1-32] AC light detection circuit (1)



KPDC0034EA

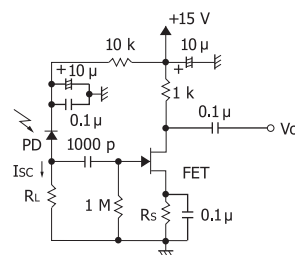
[Figure 1-33] C4890 amplifier for PIN photodiodes



AC light detection circuit (2)

This AC light detection circuit utilizes a low-capacitance PIN photodiode with a reverse voltage applied and an FET serving as a voltage amplifier [Figure 1-34]. Using a low-noise FET allows producing a small and inexpensive low-noise circuit, which can be used in light sensors for FSP (free space optics), optical remote control, etc. In Figure 1-34 the signal output is taken from the FET drain. However, to interface to a next-stage circuit having low input resistance, the signal output should be taken from the source or a voltage-follower should be added.

[Figure 1-34] AC light detection circuit (2)



KPDC0014EE

1 - 10 New approaches

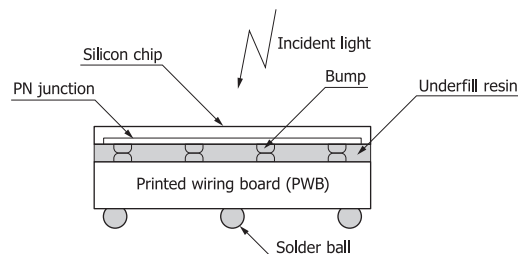
Back-illuminated photodiodes

Normal photodiodes are typically the front-illuminated type. This type has an active area, a protective film, and electrodes on the light incident surface, so the light incident surface is not flat. This may become a problem when coupling components such as a scintillator and glass. There is also an anode electrode on the light incident surface, and the silicon chip is connected to the base by wire, which takes up space within the photodiode. If using an array of multiple photodiodes having this structure, some dead space occurs between adjacent photodiode active areas, causing a problem. To resolve this problem, HAMAMATSU is developing a back-illuminated photodiode in a chip size package (CSP).

In back-illuminated photodiodes, the light incident surface is on the opposite side (back surface) of the surface where the active area and electrodes are formed, so the light incident surface can be made flat. This allows direct coupling of a scintillator or glass to the light incident surface. When using multiple photodiodes by arranging them in a tile format, the dead space between adjacent photodiodes can be minimized.

In ultraviolet detection applications, if a back-illuminated photodiode is used, there is no need for concern about sensitivity deterioration which is often caused by outgassing from the adhesive resin used to seal the light input window. Moreover, since the PN junction is formed near the surface which is mounted on a printed wiring board, deterioration caused by strong ultraviolet light is reduced.

[Figure 1-35] Back-illuminated photodiode

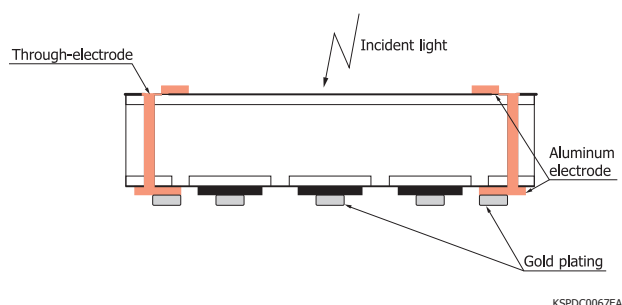


KSPDC0065EB

Through-electrode photodiodes

Through-electrode photodiodes offer the same sensitivity uniformity and response speed as normal photodiodes because a voltage can be applied to the light incident surface. This means through-electrode photodiodes can eliminate problems inherent in back-illuminated photodiodes, such as with sensitivity uniformity and response speed. Through-electrode photodiodes do not require thinning the substrate, so the manufacturing process is simple. However, their light incident surface is not completely flat because the electrode must be formed on it. Through-electrode technology can also be used in normal photodiodes (front-illuminated type) as well as in back-illuminated photodiodes.

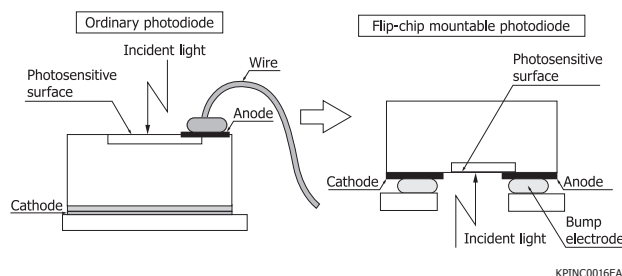
[Figure 1-36] Through-electrode photodiode



Flip-chip mountable photodiodes

Flip-chip mountable photodiodes are fabricated using MEMS technology to form the anode and cathode electrodes on the same surface. This allows designing flip-chip mountable, high-speed PIN photodiodes.

[Figure 1-37] Flip-chip mountable photodiode



2. Si APD

The APD (avalanche photodiode) is a high-speed, high-sensitivity photodiode that internally multiplies photocurrent by applying a reverse voltage. Compared to PIN photodiodes, the APD provides a higher S/N and is used in a wide variety of applications such as optical rangefinders, FSO (free space optics), and scintillation detection.

The APD can multiply a low-level light signal into a large electrical signal. However, it is not always simple to use because a high reverse voltage is needed and the multiplication ratio (gain) is temperature dependent.

This section describes Si APD features and characteristics so that users can extract maximum performance from Si APDs.

2-1 Features

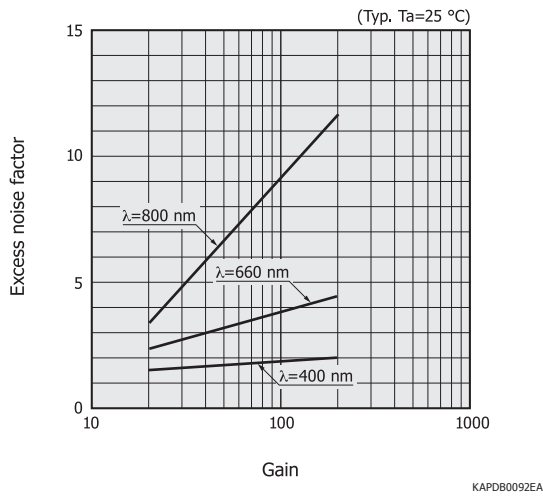
- High-speed response and high sensitivity
- Wide variety of types available
- High reliability
- Custom devices available
- Can ship to match selected specifications

Short wavelength type

Short wavelength type Si APDs are used for light detection in 400 nm band for analytical instruments and scintillation detectors, etc. These Si APDs feature extremely low noise when detecting light in the UV to visible region. They also offer excellent gain uniformity over the active area, making them easy to use even when a large active area is needed.

The HAMAMATSU S5343 is a short wavelength type Si APD operating at around 150 V and is used for optical switches, etc. The S8664 series is a low capacitance version of the S5343 and is mostly used in high energy physics experiments. We are making efforts to enhance the stability of UV sensitivity and anticipate that the Si APDs will be used in the vacuum UV region in the future.

[Figure 2-1] Excess noise factor vs. gain (S8664 series)



■ Near infrared type

Near infrared Si APDs include a low-bias operation type for 800 nm band and a low temperature coefficient type, as well as types for 900 nm laser and YAG laser.

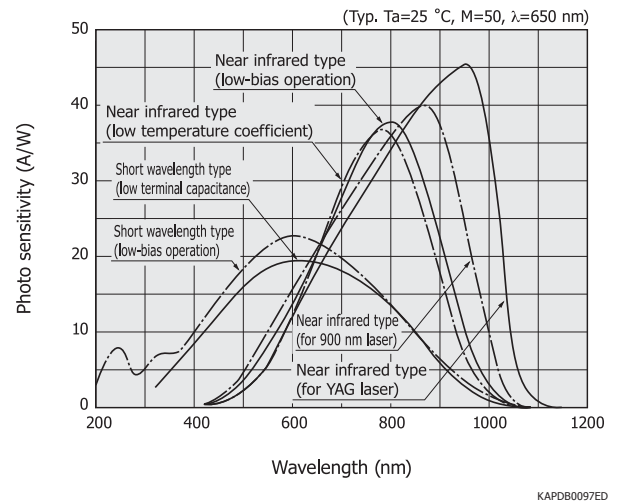
The S2381 series of the low-bias operation type features high-speed response and is controllable with a relatively low reverse voltage below 200 V. It is widely used in applications requiring high-speed response such as barcode readers, FSO, and optical rangefinders.

In the S6045 series of the low temperature coefficient type, the reverse voltage has a low temperature coefficient so the power supply does not require precise regulation even if the ambient temperature changes. This allows stable operation in a wider temperature range compared to the low-bias operation type.

The S9251 series Si APD was developed for 900 nm laser and is used in optical rangefinders, etc. The S8890 series Si APD

for YAG laser is optimized to provide high sensitivity at the 1.06 μm wavelength. Both the 900 nm laser and YAG laser types have a thick depletion layer to enhance sensitivity in the longer wavelength region. A thicker depletion layer lowers the terminal capacitance, but increases the time required for carriers to pass through the depletion layer, which limits the response characteristics in some cases. A thick depletion layer also requires a higher reverse voltage to obtain the desired gain, so the peripheral circuit design must take this high-voltage resistance into account.

[Figure 2-2] Spectral response (Si APD)



■ Multi-element type

Multi-element Si APDs have an array of active areas. The avalanche layer formed just below each active area on the APD array multiplies the light incident on the active areas. However, carriers generated outside these active areas cannot pass

[Table 2-1] HAMAMATSU Si APDs

Type		Features	Applications
Short wavelength type	Low-bias operation	Enhanced sensitivity in UV to visible region	<ul style="list-style-type: none"> Low-light-level detection Analytical instruments
	Low terminal capacitance		
Near infrared type	Low-bias operation	High sensitivity in near infrared region and low bias voltage (reverse voltage) operation	<ul style="list-style-type: none"> FSO Optical rangefinders Optical fiber communications
		Low cost and high reliability APD using surface-mount ceramic packages with the same wide operating temperature range (-20 to +85 °C) as metal package types	<ul style="list-style-type: none"> Optical rangefinders Laser radars FSO
	Low temperature coefficient	Easy voltage adjustment due to low temperature coefficient of bias voltage	<ul style="list-style-type: none"> FSO Optical rangefinders Optical fiber communications
	For 900 nm laser	Enhanced sensitivity in 900 nm band	<ul style="list-style-type: none"> Optical rangefinders Laser radars
	For YAG laser	Enhanced sensitivity in 1.6 μm band (YAG laser)	<ul style="list-style-type: none"> YAG laser detection

through the avalanche layer so their signal is small. This means that APD arrays have lower crosstalk than photodiode arrays because of their gain.

[Figure 2-3] Internal structure (multi-element Si APD)

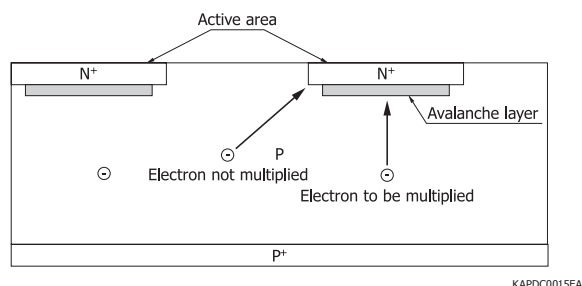
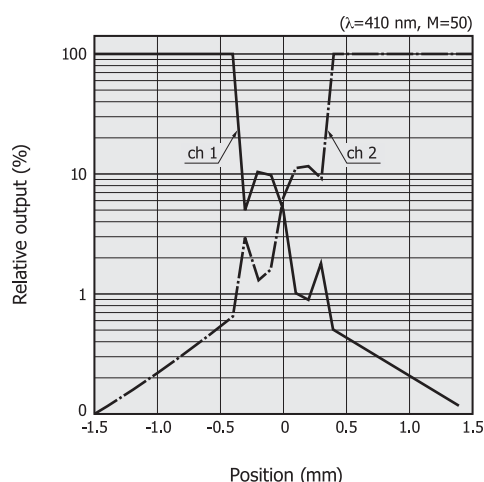


[Figure 2-4] Crosstalk (S8850, element gap: 0.7 μm, typical example)



2-2 Principle of avalanche multiplication

When light enters a photodiode, electron-hole pairs are generated if the light energy is higher than the band gap energy. The ratio of the number of generated electron-hole pairs to the number of incident photons is called the quantum efficiency (QE), commonly expressed in percent (%). The mechanism by which carriers are generated inside an APD is the same as in a photodiode, but the APD has a function to multiply the generated carriers.

When electron-hole pairs are generated in the depletion layer of an APD with a reverse voltage applied to the PN junction, the electric field created across the PN junction causes the electrons to drift toward the N⁺ side and the holes to drift toward the P⁺ side. The drift speed of these electron-hole pairs or carriers depends on the electric field strength. However, when the electric field is increased, the carriers are more likely to collide with the crystal lattice so that the drift speed of each carrier becomes saturated at a certain speed. If the reverse voltage is increased even further, some carriers that escaped collision with the crystal lattice will have a great deal of energy. When these

carriers collide with the crystal lattice, ionization takes place in which electron-hole pairs are newly generated. These electron-hole pairs then create additional electron-hole pairs in a process just like a chain reaction. This is a phenomenon known as avalanche multiplication.

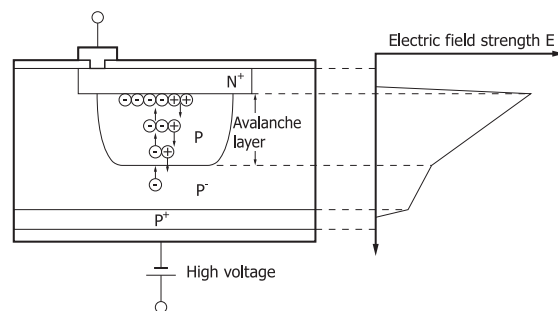
The number of electron-hole pairs generated during the time that a carrier moves a unit distance is referred to as the ionization rate. Usually, the ionization rate of electrons is defined as “α” and that of holes as “β.” These ionization rates are important factors in determining the multiplication mechanism. In the case of silicon, the ionization rate of electrons is larger than that of holes (α > β), so the electrons contribute more to the multiplication. The ratio of β to α is called the ionization rate ratio (k) and is used as a parameter to indicate APD noise.

$$k = \frac{\beta}{\alpha} \dots\dots\dots (17)$$

2-3 Gain vs. reverse voltage characteristics

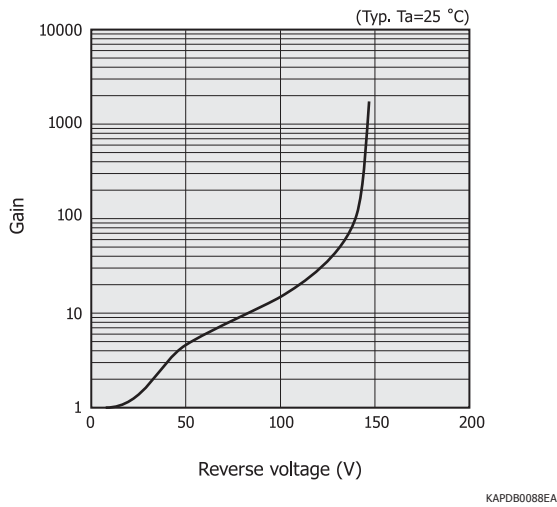
The APD gain is determined by the ionization rate, and the ionization rate depends on the electric field across the depletion layer. The internal structure of HAMAMATSU APDs is designed so that ionization occurs efficiently. The near infrared type Si APD has a so-called reach-through structure in which the avalanche layer is formed so that the electric field is easily concentrated on the PN junction.

[Figure 2-5] Schematic diagram of avalanche multiplication (near infrared type Si APD)



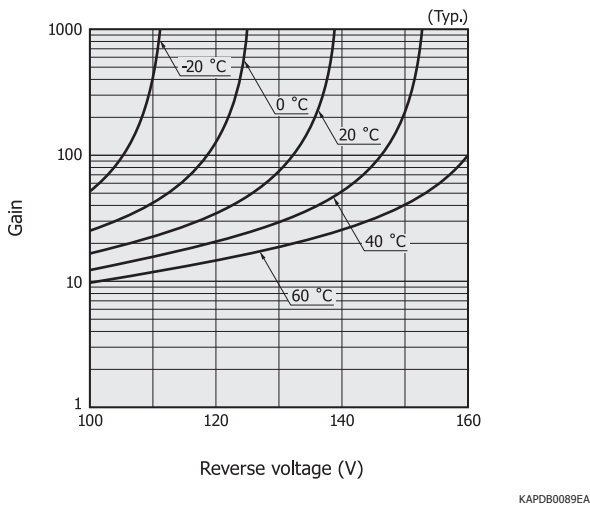
When a reverse voltage is applied to the PN junction, the electric field in the depletion layer increases so avalanche multiplication occurs. As the reverse voltage is increased, the gain increases and eventually reaches the breakdown. Figure 2-6 shows the relation between the gain and reverse voltage for HAMAMATSU Si APD S2382.

[Figure 2-6] Gain vs. reverse voltage (S2382)



The APD gain also has temperature-dependent characteristics. As the temperature rises, the crystal lattice vibrates more heavily, increasing the possibility that the accelerated carriers may collide with the lattice before reaching a sufficiently large energy level and making it difficult for ionization to take place. Therefore, the gain at a certain reverse voltage becomes small as the temperature rises. To obtain a constant output, the reverse voltage must be adjusted to match changes in temperature or the APD temperature must be kept constant.

[Figure 2-7] Temperature characteristics of gain (S2382)



When an APD is used near the breakdown voltage, a phenomenon occurs in which the output photocurrent is not proportional to the amount of incident light. This is because a voltage drop occurs due to current flowing through the series resistance and load resistance in the APD, reducing the voltage applied to the avalanche layer as the photocurrent increases.

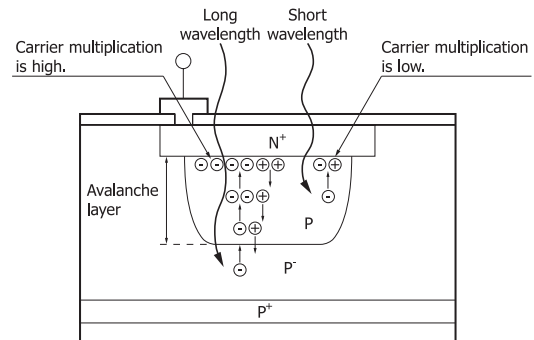
2 - 4 Spectral response

Spectral response characteristics of APDs are almost the same as those of normal photodiodes if a reverse voltage is

not applied. When a reverse voltage is applied, the spectral response curve will change.

The depth to which light penetrates in the silicon depends on the wavelength. The depth to which shorter-wavelength light can reach is shallow, so carriers are generated near the surface. In contrast, longer-wavelength light generates carriers at deeper positions. The avalanche multiplication occurs when the carriers pass through the high electric field near the PN junction. In the case of silicon, the ionization rate of electrons is high, so it must have a structure that injects the electrons to the avalanche layer. In Figure 2-8, for example, light reaches the P-layer and the generated carriers (electrons) are accelerated by the electric field toward the N^+ -layer to cause multiplication. Satisfactory gain characteristics can therefore be obtained when detecting long-wavelength light that reaches the P-layer.

[Figure 2-8] Schematic of cross section (near infrared type Si APD)



Which of short-wavelength light or long-wavelength light is more efficiently multiplied depends on the APD structure. Figures 2-9 and 2-10 show the wavelength dependence of spectral response characteristics and gain for the short wavelength type Si APD S5343 and near infrared type Si APD S2383.

[Figure 2-9] Spectral response

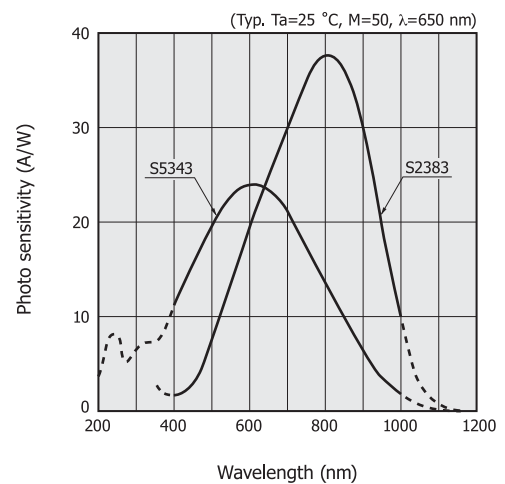
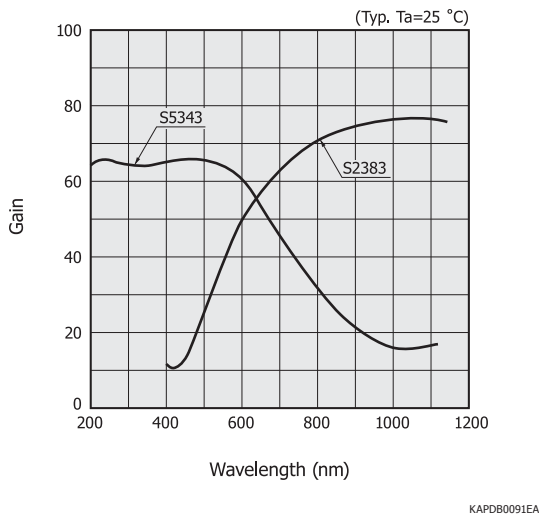


[Figure 2-10] Gain vs. wavelength



2-5 Time response characteristics

Major factors that determine the response speed of photodiodes are the CR time constant and the carrier transit time (drift time) in the depletion layer. The cut-off frequency $f_c(\text{CR})$ determined by the CR time constant is given by equation (18).

$$f_c(\text{CR}) = \frac{1}{2\pi C_t R_L} \dots\dots\dots (18)$$

C_t : terminal capacitance
 R_L : load resistance

To improve photodiode response speeds, the terminal capacitance should be reduced, for example by making the active area smaller and the depletion layer thicker. The relation between the cut-off frequency $f_c(\text{CR})$ and the rise time t_r is expressed by equation (19).

$$t_r = \frac{0.35}{f_c(\text{CR})} \dots\dots\dots (19)$$

If the depletion layer is widened, the drift time cannot be ignored. The transit speed (drift speed) in the depletion layer begins to saturate when the electric field strength reaches the vicinity of 10^4 V/cm, and the saturated drift speed at this point will be approx. 10^7 cm/s. Ionization occurs when the carriers that have moved to the avalanche layer generate electron-hole pairs. However, since the holes move in the direction opposite to that of the electrons, the drift time in the APD becomes longer than that in PIN photodiodes. If we let the drift time be t_{rd} , the cut-off frequency $f_c(t_{\text{rd}})$ determined by the drift time is given by equation (20).

$$f_c(t_{\text{rd}}) = \frac{0.44}{t_{\text{rd}}} \dots\dots\dots (20)$$

Making the depletion layer thicker to reduce the capacitance also lengthens the drift time, so it is essential to consider both cut-off frequencies, $f_c(\text{CR})$ determined by the CR time constant

and $f_c(t_{\text{rd}})$ determined by the transit time.

The carriers passing through the avalanche layer repeatedly collide with the crystal lattice, so a longer time is required to move a unit distance in the avalanche layer than the time required to move a unit distance in areas outside the avalanche layer. The time required to pass through the avalanche layer becomes longer as the gain is increased. If an APD is used at a gain of several hundred times, the time needed for multiplication (multiplication time) might be a problem.

The factors that determine the response speed are the CR time constant, drift time, multiplication time, and a time delay which is caused by diffusion current of carriers from outside the depletion layer. This time delay is sometimes as large as a few microseconds and appears more remarkably in cases where the depletion layer is not extended enough with respect to the penetration depth of the incident light into the silicon. To ensure high-speed response, it is also necessary to take the wavelength to be used into account and to apply a reverse voltage that sufficiently widens the depletion layer.

When the incident light level is high and the resulting photocurrent is large, the attractive power of electrons and holes in the depletion layer serves to cancel out the electric field, making the carrier drift speed slower and impairing the time response. This phenomenon is called the space charge effect and tends to occur especially when the incident light is interrupted.

2-6 Noise characteristics

As long as the reverse voltage is constant, the APD gain is the average of each carrier's multiplication. However, the ionization rate is not uniform and has statistical fluctuations. Multiplication noise known as excess noise is therefore added during the multiplication process. The APD shot noise (I_n) becomes larger than the PIN photodiode shot noise and is expressed by equation (21).

$$I_n^2 = 2q (I_L + I_{\text{dg}}) B M^2 F + 2q I_{\text{ds}} B \dots\dots\dots (21)$$

q : electron charge
 I_L : photocurrent at $M=1$
 I_{dg} : dark current component multiplied
 B : bandwidth
 M : multiplication ratio (gain)
 F : excess noise factor
 I_{ds} : dark current component not multiplied

The excess noise factor (F) can be expressed by the ratio of the electron/hole ionization rate ratio (k), as shown in equation (22).

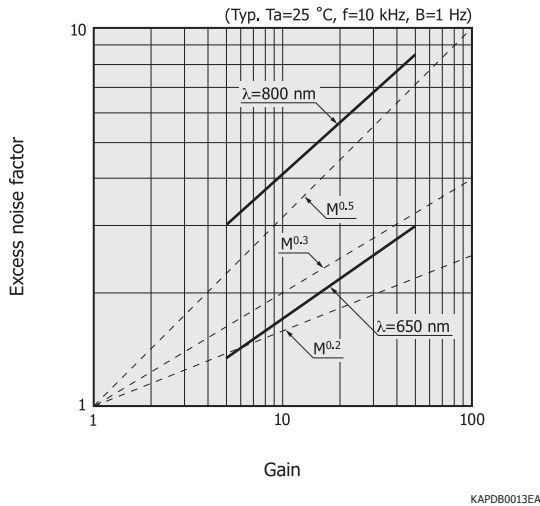
$$F = M k + (2 - \frac{1}{M}) (1 - k) \dots\dots\dots (22)$$

Equation (22) shows the excess noise factor when electrons are injected into the avalanche layer. To evaluate the excess noise factor when holes are injected into the avalanche layer, k in equation (22) should be substituted by $1/k$.

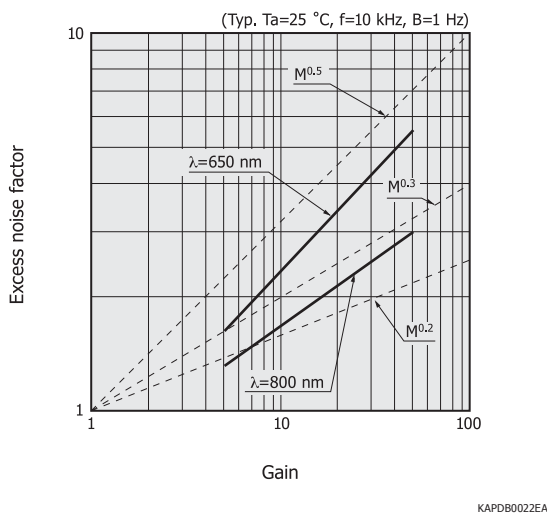
As described in section 2-4, “Spectral response,” the gain is wavelength dependent. Likewise, the excess noise also has wavelength dependence. There are different types of APDs, which exhibit low noise at short wavelengths or at long wavelengths. Figure 2-11 shows excess noise characteristics.

[Figure 2-11] Excess noise factor vs. gain

(a) Short wavelength type (low-bias operation)



(b) Near infrared type (low-bias operation)



The excess noise factor (F) can also be approximated as $F=M^x$ (x: excess noise index) because the equation for shot noise can be expressed in the form of $I_n^2=2q I_L B M^{2+x}$.

As explained, APDs generate noise due to the multiplication process, so excess noise increases as the gain becomes higher. The photocurrent generated by signal light is also amplified according to the gain, so there is a gain at which the S/N is maximized. The S/N for an APD can be expressed by equation (23).

$$S/N = \frac{I_L^2 M^2}{2q (I_L + I_{dg}) B M^2 F + 2q B I_{ds} + \frac{4k T B}{R_L}} \dots\dots\dots (23)$$

$2q (I_L + I_{dg}) B M^2 F + 2q B I_{ds}$: shot noise

$\frac{4k T B}{R_L}$: thermal noise

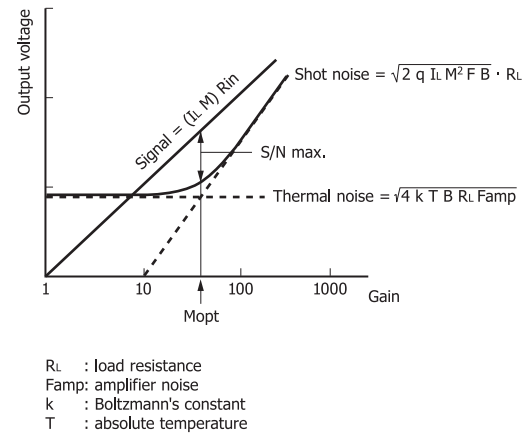
k : Boltzmann's constant

T : absolute temperature

R_L : load resistance

In PIN photodiode operation, using a larger load resistance reduces thermal noise, but this also slows the response speed. Therefore, it is not practical to reduce thermal noise and, in most cases, the lower limit of light detection is determined by thermal noise. In APD operation, the signal can be multiplied without increasing the total noise until the shot noise reaches a level equal to the thermal noise, thus resulting in an improved S/N while maintaining the high-speed response. This behavior is shown in Figure 2-12.

[Figure 2-12] APD noise characteristics



In this case, the optimum gain (M_{opt}) is obtained under the conditions that maximize the S/N described in equation (23). If I_{ds} can be ignored, the optimum gain is given by equation (24).

$$M_{opt} = \left[\frac{4k T}{q (I_L + I_{dg}) \times R_L} \right]^{\frac{1}{2+x}} \dots\dots\dots (24)$$

2-7 Connection to peripheral circuits

APDs can be handled in the same manner as normal photodiodes except that a high reverse voltage is required. However, the following precautions should be taken because APDs are operated at a high voltage.

APD power consumption is the product of the signal input \times sensitivity \times gain \times reverse voltage, and it is considerably larger than that of PIN photodiodes. So there is a need to add a protective resistor and to install a current limiting circuit to the bias circuit.

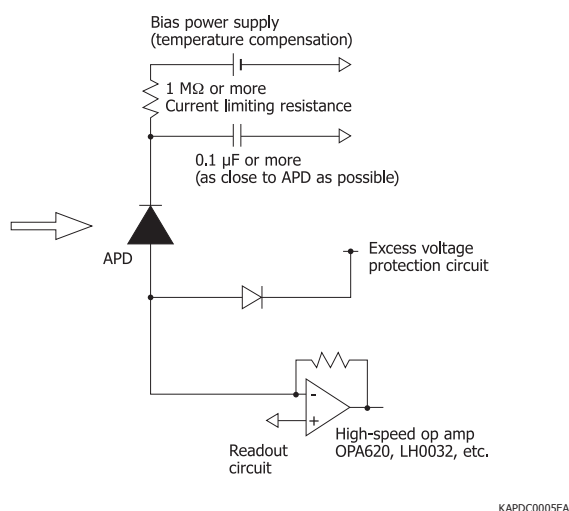
A low-noise readout circuit usually has high input impedance so the first stage might be damaged by excess voltage. To

prevent this, a protective circuit should be connected to divert any excess input voltage to the power supply voltage line.

APD gain changes with temperature. To use an APD over a wide temperature range, the reverse voltage must be controlled to match the temperature changes or the APD temperature must be maintained at a constant level.

When detecting low-level light signals, the lower detection limit is determined by the shot noise. If background light enters the APD, then the S/N may deteriorate due to shot noise from background light. In this case, effects from the background light must be minimized by using optical filters, improving laser modulation, and/or restricting the angle of view.

[Figure 2-13] Connection example



APD modules

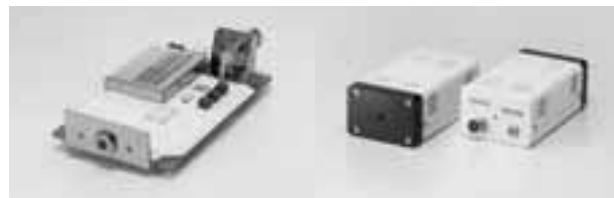
APD modules are high-speed, high-sensitivity photodetectors using an APD. APD modules consist of an APD, a low noise amplifier, and a bias power supply assembled in a compact configuration. By simply connecting to a low-voltage DC power supply, APD modules can detect light with a good S/N which is dozens of times higher than PIN photodiodes. APD modules help users evaluate and fabricate their high-performance system using an APD.

Figure 2-15 shows the block diagram of the C5331 series APD module. This module is designed with the precautions described in section 2-7, “Connection to peripheral circuits,” thus allowing highly accurate photometry.

For more detailed information about APD modules, refer to “4. APD modules” in Chapter 10, “Module products.”

[Figure 2-14] APD modules

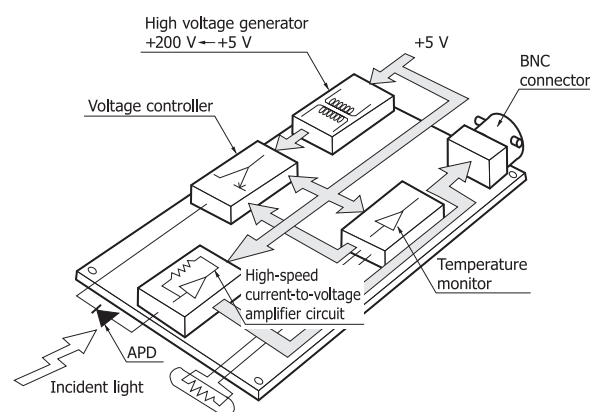
(a) Standard type C5331 series (b) TE-cooled type C4777 series



(c) High-speed type C5658 (d) High-stability type C10508



[Figure 2-15] Block diagram (C5331 series)



2-8 APD for photon counting

The light we usually see consists of a stream of light particles (photons) that produce a certain level of brightness. When this brightness falls to a very low level, the incoming photons are separate from each other. The technique to measure low-level light by counting the number of photons is called “photon counting.”

APDs exhibit an internal multiplication of carriers when a high reverse voltage is applied, and they have been used to detect

[Table 2-2] HAMAMATSU APD modules

Type	Features
Standard type	Contains a near infrared or short wavelength type APD. FC/SMA connector types are also available.
High-sensitivity type	High gain type for low-light-level detection
High-stability type	Digital temperature-compensation, high-stability APD module
High-speed type	Can be used in a wide-band frequency range (up to 1 GHz)
TE-cooled type	High-sensitivity type for ultra-low light detection. Stability is greatly improved by thermoelectric cooling.

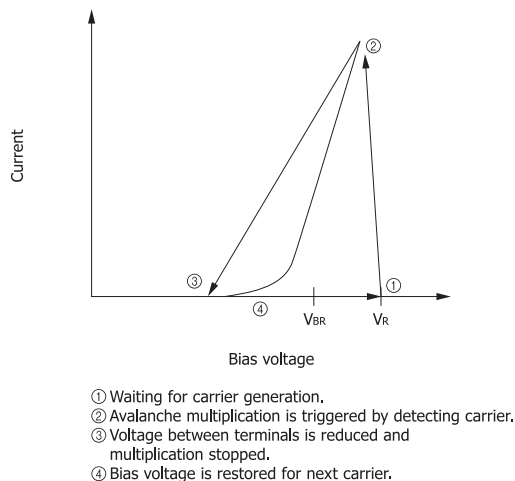
low-level light. Normally, APDs are used at a gain from several dozen to several hundred times. When the reverse voltage is set higher than the breakdown voltage, a very large gain can be obtained. Operating an APD under this condition is called “Geiger mode,” and the APD becomes capable of detecting single photons. HAMAMATSU provides a new type of photon-counting device made up of multiple APD pixels that operate in Geiger mode, which is named “MPPC.” (See “3. MPPC” in Chapter 2, “Si photodiodes.”)

Geiger-mode operation

When the reverse voltage applied to an APD is increased higher than the breakdown voltage, the internal electric field becomes extremely high. Under this condition, when a carrier is injected into the avalanche layer, a very large pulse is generated as a result of avalanche multiplication. If the carrier is generated by light, the pulse generation should occur at the timing when each photon enters the APD. Then, when the reverse voltage is decreased below the breakdown voltage, the multiplication ceases (quenching) and the bias voltage is restored. In photon counting, the number of pulses generated by each photon is counted to measure the light level.

In this operation, the extent to which the reverse voltage is set higher than the breakdown voltage significantly affects the characteristics.

[Figure 2-16] Quenching



Photon-counting characteristics

(1) Photon detection efficiency

Photon detection efficiency is a measure of what percent of the incident photons were detected. Because not all generated carriers will create pulses large enough to be detected, photon detection efficiency is lower than quantum efficiency. Photon detection efficiency increases as the reverse voltage is increased.

(2) Dark count

Output pulses are produced not only by photon-generated carriers but also by thermally-generated dark current carriers. These dark current pulses are measured as dark count which then causes detection errors. Although increasing the reverse voltage improves photon detection efficiency, it also increases the dark count. The dark count can be reduced by lowering the temperature.

(3) Afterpulse

Afterpulses are spurious pulses following the true signal, which occur when the generated carriers are trapped by crystal defects and then released at a certain time delay. Afterpulses also cause detection errors. The lower the temperature, the higher the probability that carriers may be trapped by crystal defects, so afterpulses will increase.

(4) Residual signal

In photon-counting measurements, a pulse is generated by one carrier. If there is a delayed carrier flowing from outside the depletion layer, it will also be detected as a signal pulse. This acts as a residual signal and causes detection errors.

Photon-counting measurement circuit

In photon counting, the reverse voltage is lowered by detecting a carrier, and is then again restored to a level higher than the breakdown voltage after multiplication is quenched. This operation is repeated using a quenching circuit [Figure 2-16]. There are two types of quenching circuits: passive quenching circuit and active quenching circuit.

(1) Passive quenching circuit

A passive quenching circuit is simple, as shown in Figure 2-17. A multiplied pulse current is quenched by a voltage drop across both ends of a high load resistance. Incidentally, an MPPC has a structure in which multiple passive quenching circuits are formed.

[Figure 2-17] Passive quenching circuit

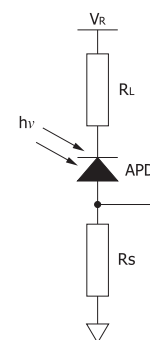
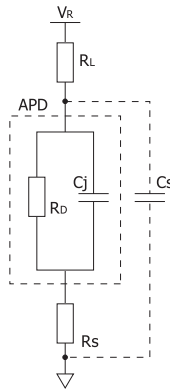


[Figure 2-18] Equivalent circuit (passive quenching circuit)



KAPDC0019EB

A high reverse voltage V_R is applied to the APD through a load resistance R_L of about 100 k Ω . The APD itself has the internal resistance R_D and diode capacitance C_J , and also a stray capacitance C_S is added. As long as no carriers are present, the terminal capacitance and stray capacitance are charged and V_R is applied to the APD. When an avalanche multiplication is triggered, a current begins to flow through R_L , and the reverse voltage decreases and then the diode current decreases. As the current becomes extremely small, the capacitances are recharged through R_L and the diode reverse voltage is restored to V_R , preparing for the next pulse.

The quenching time (T_q) is expressed by equation (25).

$$T_q = (C_J + C_S) \frac{R_D \times R_L}{R_D + R_L} \approx (C_J + C_S) R_D \quad \text{..... (25)}$$

The time (T_R) required for the voltage to restore itself is given by equation (26).

$$T_R = (C_J + C_S) R_L \quad \text{..... (26)}$$

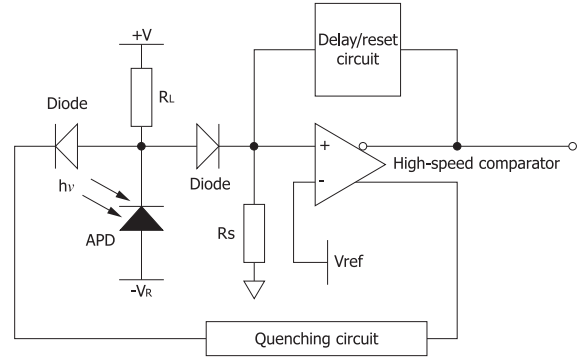
If photons enter the APD before the reverse voltage is restored, they will not be detected. This period is the dead time and affects the linearity.

The output pulse can be obtained through R_S .

(2) Active quenching circuit

In the basic operation of an active quenching circuit, a multiplied current pulse is detected and fed back to the reverse voltage to reduce it, so that the gain is forced to be low.

[Figure 2-19] Active quenching circuit



KAPDC0020EA

When a pulse is detected by the high-speed comparator, the APD reverse voltage is switched to the breakdown voltage or less by the quenching circuit. The delay/reset circuit then returns the comparator input to a voltage higher than V_{ref} , and the APD is separated from the quenching circuit and delay/reset circuit. Then the APD is recharged through the load resistance R_L and enabled to detect the next pulse. The active quenching circuit therefore has an advantage that it can control and shorten the dead time. It also has an effect of reducing afterpulses while the avalanche multiplication is stopped, by generating a trigger pulse in a certain time period to lower the bias voltage.

2-9 New approaches

APDs are not so easy to use because they need a high reverse voltage and their gain is temperature dependent. HAMAMATSU is developing APDs that will make gain control easier, such as those operating on a low voltage or having a built-in preamp to allow simple adjustment of applied voltage. Downsizing of APD chips is expected to give excellent cost-performance and to expand the range of applications. We are also developing APDs with optical filters integrated into the chip or package to minimize disturbing light noise. These products also have great potential for use in compact rangefinders and inter-vehicle distance sensors, etc.

HAMAMATSU is also making progress in developing large-area APDs and APD arrays. Our APD arrays offer superb sensitivity uniformity and help make PET (positron emission tomography) equipment more compact and energy-efficient. Another advantage that APD arrays offer is that they are unaffected by magnetic fields, so they can be used in hybrid equipment combining PET and MRI (magnetic resonance imaging).

HAMAMATSU is also applying MEMS technology to developing new APDs that are compact yet deliver high-speed response. Other APDs under development include back-illuminated APDs with high sensitivity in the short-wavelength region and APDs with superb energy resolution and high S/N in the high energy domain such as for X-rays, etc.

3. MPPC

The MPPC (multi-pixel photon counter) is one of the devices called Si-PM (silicon photomultiplier). It is a new type of photon-counting device using multiple APD (avalanche photodiode) pixels operating in Geiger mode. Although the MPPC is essentially an opto-semiconductor device, it has excellent photon-counting capability and can be used in various applications for detecting extremely weak light at the photon-counting level.

The MPPC operates on a low voltage and features a high multiplication ratio (gain), high photon detection efficiency, fast response, excellent time resolution, and wide spectral response range, so it delivers the high-performance level needed for photon counting. The MPPC is also immune to magnetic fields, highly resistant to mechanical shocks, and will not suffer from “burn-in” by input light saturation, which are advantages unique to solid-state devices. The MPPC therefore has a potential for replacing conventional detectors used in photon counting up to now.

Since the MPPC is an easy-to-operate, high-performance detector, it is suitable for photon counting where extreme high sensitivity is required from the photodetectors. The MPPC is a promising device for use in a wide range of fields including fluorescence analysis, fluorescence lifetime measurement, biological flow cytometry, confocal microscopes, biochemical sensors, bioluminescence analysis, and single molecule detection.

3-1 Features

- Excellent photon-counting capability (excellent detection efficiency versus number of incident photons)
- Room temperature operation
- Low voltage (below 100 V) operation
- High gain: 10^5 to 10^6
- Excellent gain uniformity over active area
- Excellent time resolution
- Insensitive to magnetic fields
- Small size
- Simple readout circuit operation
- Spectral response matching scintillator emission wavelengths (peak sensitivity wavelength: 440 nm typ.)
- Choice of packages according to application (custom devices available)
- MPPC modules available (sold separately)

3-2 Operating principle

Geiger mode

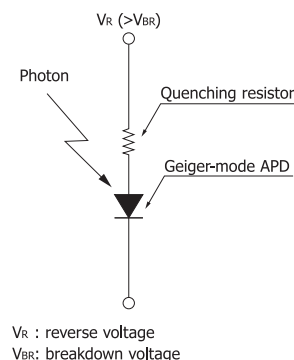
Geiger mode is a method for operating an APD at a reverse voltage higher than the breakdown voltage. A high electric field is produced in the APD during Geiger mode so that a discharge (Geiger discharge) occurs even from a weak light input. The electron gain at this point is as high as 10^5 or 10^6 , and the magnitude of the output current is constant regardless of the number of input photons.

Connecting a quenching resistor to an APD operated in Geiger mode creates an effect that stops the APD avalanche multiplication in a short time, acting as a circuit that outputs a pulse at a constant level when it detects a photon.

[Table 3-1] APD operation mode

Operation mode	Reverse voltage	Gain
Normal mode	Below breakdown voltage	Dozens to several hundred
Geiger mode	Above breakdown voltage	10^5 to 10^6

[Figure 3-1] Geiger-mode APD and quenching resistor

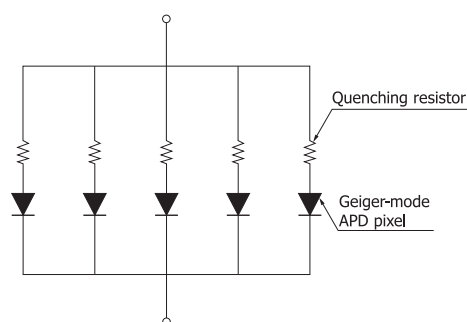


KAPDC0023EA

Principle of MPPC operation

An MPPC has a structure in which combinations of a Geiger-mode APD pixel and a quenching resistor are connected in parallel and arranged in two dimensions [Figure 3-2].

[Figure 3-2] MPPC equivalent circuit



KAPDC0029EA

Each APD pixel independently detects a photon and determines whether or not one photon has entered it. The output produced when one or more photons have entered an APD pixel is constant regardless of the number of input photons. This means that each APD pixel only provides information on whether or not it received a photon. Since an MPPC consists of multiple APD pixels, the MPPC output is the sum of the outputs from multiple APD pixels. This MPPC output indicates the number of APD pixels that have detected a photon.

A quenching resistor is connected to each APD pixel to allow the output current to flow through it. Since all APD pixels are connected to one readout channel, the output pulses from the APD pixels overlap each other, creating a large pulse. By measuring the height or electric charge (Q_{out}) of this pulse, the number of photons detected by the MPPC can be estimated.

$$Q_{out} = C \times (V_R - V_{BR}) \times N_{fired} \quad (27)$$

Q_{out} : electric charge of pulse
 C : capacitance of an APD pixel
 V_R : reverse voltage
 V_{BR} : breakdown voltage
 N_{fired} : number of APD pixels that detected photons

The MPPC has excellent photon-counting capability. Connecting the MPPC to an amplifier will show sharp waveforms on an oscilloscope according to the number of detected photons.

Figure 3-3 shows an overlap display of pulse waveforms obtained when low-level light was incident on the MPPC. As can be seen, the pulse height varies according to the number of detected photons. The fact that the individual pulse waveforms are clearly separate from each other proves there is little variation between the gains of APD pixels making up the MPPC.

[Figure 3-3] Pulse waveforms when using amplifier (120 times)
 (active area: 1 mm sq, pixel size: 50 μ m sq)

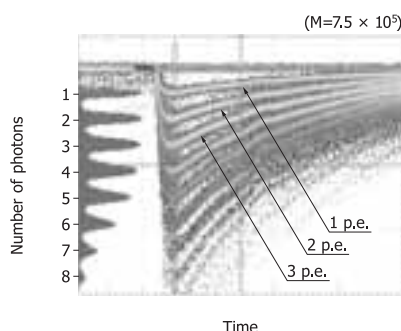
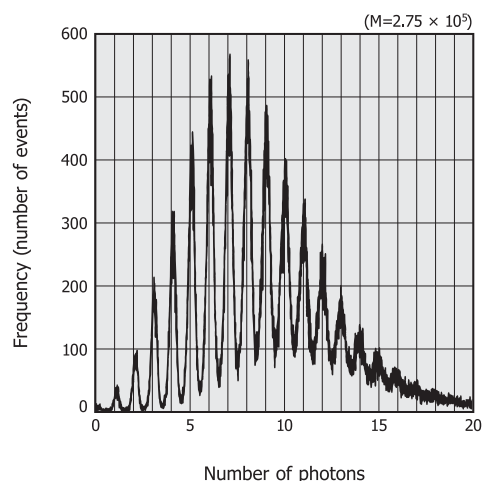


Figure 3-4 is a pulse height spectrum showing the graphical distribution of electric charges obtained within a certain time period by measuring the MPPC output with a charge amplifier.

[Figure 3-4] Pulse height spectrum when using charge amplifier
 (active area: 1 mm sq, pixel size: 25 μ m sq)



KAPDB0133EA

3-3 Gain

Definition of gain

The MPPC gain is defined as the charge (Q) of the pulse generated when an APD pixel detects a photon, divided by the charge of one electron (1.6×10^{-19} C).

$$\text{Gain} = \frac{Q}{q} \quad (28)$$

The charge Q in equation (28) depends on the reverse voltage (V_R) and breakdown voltage (V_{BR}) and is expressed by equation (29).

$$Q = C \times (V_R - V_{BR}) \quad (29)$$

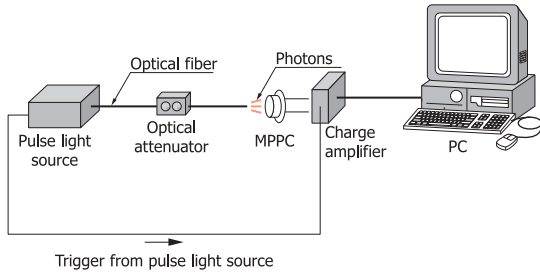
C : capacitance of an APD pixel

Because the APD pixel capacitance is constant, the gain changes linearly with respect to the " $V_R - V_{BR}$ " value.

Gain measurement

Gain can be estimated from the output charge of the MPPC that detected photons. The gain varies with the reverse voltage applied to the MPPC. Figure 3-5 shows a connection example for gain measurement.

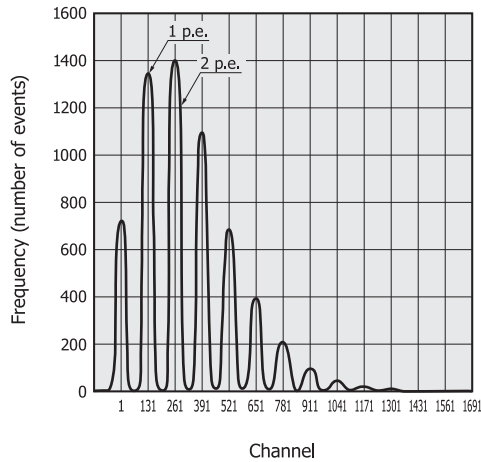
[Figure 3-5] Gain measurement connection example
(using charge amplifier)



KAPDC0031EA

Pulsed light is sufficiently reduced in intensity by the optical attenuator and is irradiated onto the MPPC. The MPPC output is then processed by the PC to obtain a frequency distribution for that output charge. An output result is obtained as shown in Figure 3-6.

[Figure 3-6] Frequency distribution example of output charge



KAPDB0136EA

Figure 3-6 represents the amount of digitized output charge from the MPPC. The ADC rate (electric charge per channel) in Figure 3-6 is 0.382 fC/ch. The output charge is increasing to the right on the horizontal axis. The vertical axis is the frequency (number of events) at each output charge. The distribution curves shown in Figure 3-6 are clearly separate, indicating output results characteristic of the MPPC. The peak of each curve starting from the left shows: the pedestal, 1 p.e. (one photon equivalent), 2 p.e., 3 p.e., etc. This example indicates that the MPPC detected photons with a distribution centered at one or two photons.

The distance between adjacent peaks exactly equals the output charge of one detected photon. The gain is therefore expressed by equation (30).

$$\text{Gain} = \frac{\text{Number of channels between two peaks} \times \text{ADC rate}}{q} \dots (30)$$

q : electron charge

The number of channels between two adjacent peaks is 130 ch in Figure 3-6, the ADC conversion rate is 0.382 fC/ch, and the

charge of an electron is 1.6×10^{-19} C, so the gain becomes as follows:

$$\frac{130 \times 0.382 \times 10^{-15}}{1.6 \times 10^{-19}} = 3.10 \times 10^5$$

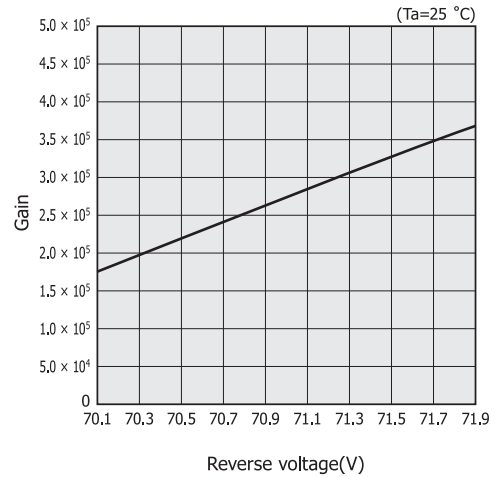
To enhance accuracy, the gain is calculated by averaging the peak values between multiple channels.

Gain linearity

The MPPC gain has an excellent linearity near the recommended operating voltage.

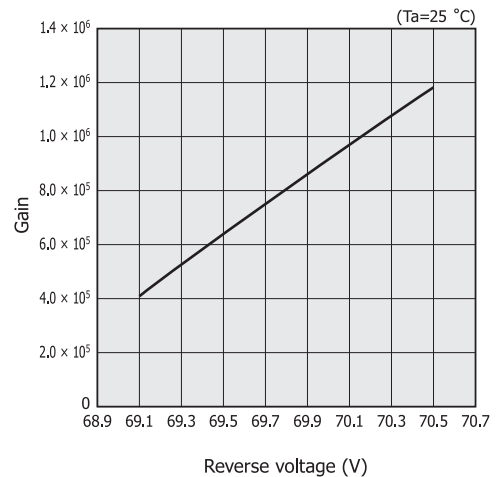
[Figure 3-7] Gain vs. reverse voltage (typical example)

(a) Active area: 1 mm sq, pixel size: 25 μm sq



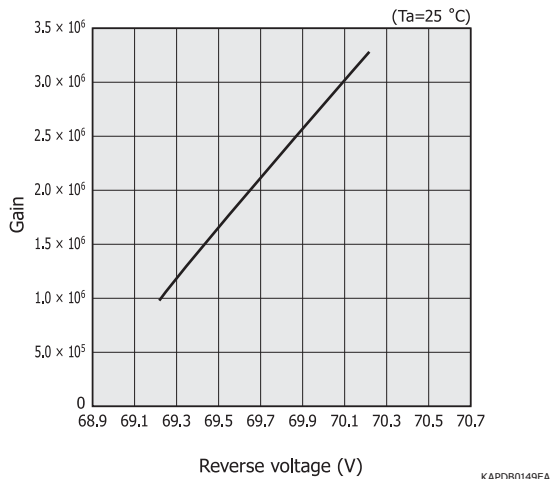
KAPDB0131EB

(b) Active area: 1 mm sq, pixel size: 50 μm sq



KAPDB0148EA

(c) Active area: 1 mm sq, pixel size: 100 μm sq



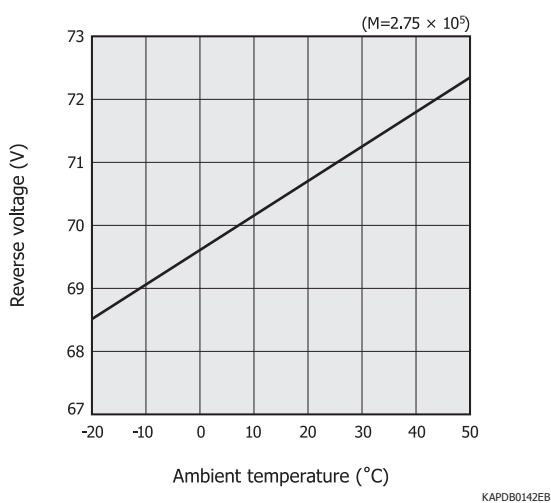
Temperature characteristics of gain

As with the APD, the MPPC gain is also temperature dependent. As the temperature rises, the crystal lattice vibrations become stronger. This increases the probability that carriers may strike the crystal before the accelerated carrier energy has become large enough, making it difficult for ionization to occur. Therefore, the gain at a fixed reverse voltage drops as the temperature rises. In order to obtain a stable output, it is essential to change the reverse voltage according to the temperature or keep the device at a constant temperature.

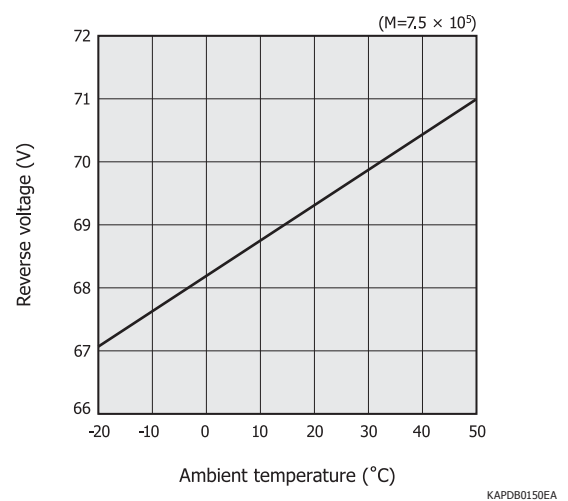
Figure 3-8 shows the reverse voltage required to keep the gain constant when the ambient temperature varies. If the ambient temperature rises, the reverse voltage must be increased at a rate of approx. 56 mV/°C.

[Figure 3-8] Reverse voltage vs. ambient temperature (typical example)

(a) Active area: 1 mm sq, pixel size: 25 μm sq



(b) Active area: 1 mm sq, pixel size: 50 μm sq



(c) Active area: 1 mm sq, pixel size: 100 μm sq

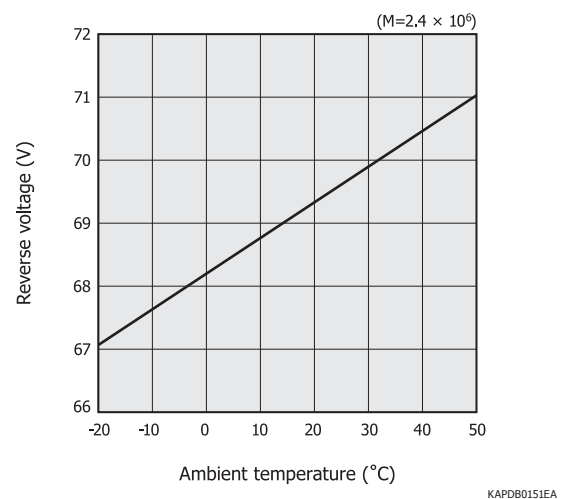
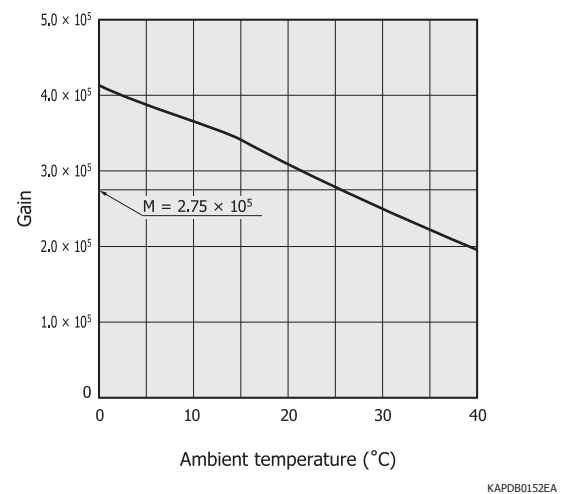


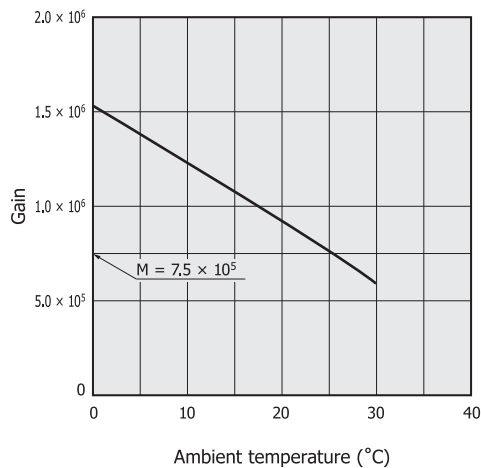
Figure 3-9 shows changes in the gain as the ambient temperature changes while the reverse voltage is fixed.

[Figure 3-9] Gain vs. ambient temperature

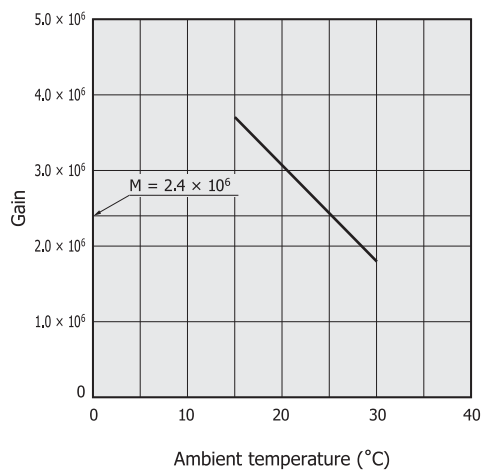
(at fixed reverse voltage, typical example)

(a) Active area: 1 mm sq, pixel size: 25 μm sq



(b) Active area: 1 mm sq, pixel size: 50 μm sq

KAPDB0153EA

(c) Active area: 1 mm sq, pixel size: 100 μm sq

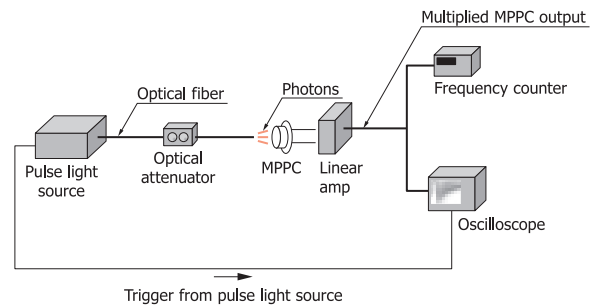
KAPDB0154EA

3-4 Dark count

The MPPC is a solid-state device, so it generates noise due to thermal excitation. The dark current in the MPPC is amplified and output as dark pulses. The number of dark pulses per second is termed the dark count [units: cps (count per second)]. Since the MPPC operates in Geiger mode, the noise component is also amplified and cannot be distinguished from the original photon detection signal. This noise occurs randomly so its frequency (dark count) is a crucial parameter in determining MPPC device characteristics. The dark count varies depending on the reverse voltage and ambient temperature.

The dark pulse in the MPPC is output as a pulse of the 1 p.e. level, making it difficult to discern a dark pulse from the output obtained when one photon is detected. However, it is very unlikely that dark pulses at 2 p.e., 3 p.e., or 4 p.e. level are detected. This means that, when a certain amount of photons are input and detected, the effects of dark pulses can be virtually eliminated by setting a proper threshold level. If the time at which light enters the MPPC is known, the effects of dark pulses during measurement can be further reduced by setting an appropriate gate time.

[Figure 3-10] Dark count measurement connection example



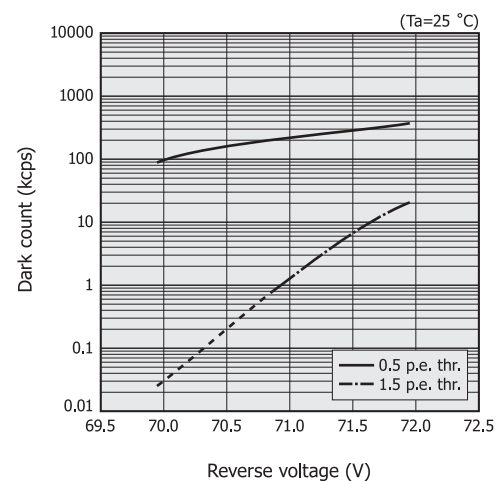
KAPDC0032EB

Dark count and crosstalk

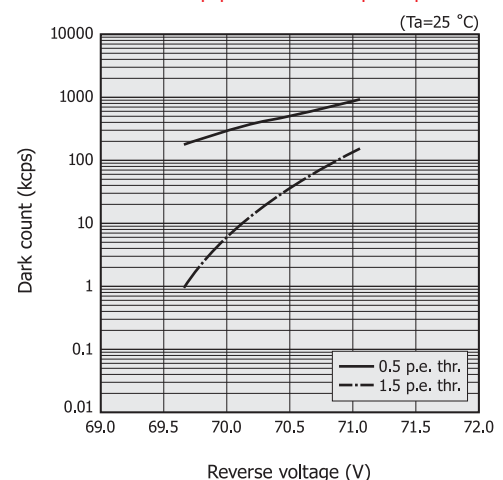
The number of output pulses measured with no light incident on the MPPC under the condition that the threshold is set at "0.5 p.e." is usually viewed as a dark count (0.5 p.e. thr.). In some cases, the dark count (1.5 p.e. thr.) measured at a threshold set at "1.5 p.e." is used to evaluate crosstalk.

Typical dark count examples

[Figure 3-11] Dark count vs. reverse voltage

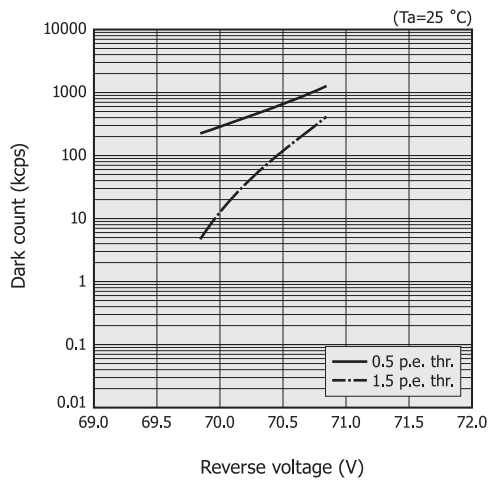
(a) Active area: 1 mm sq, pixel size: 25 μm sq

KAPDB0132EB

(b) Active area: 1 mm sq, pixel size: 50 μm sq

KAPDB0155EA

(c) Active area: 1 mm sq, pixel size: 100 μm sq



(c) Active area: 1 mm sq, pixel size: 100 μm sq

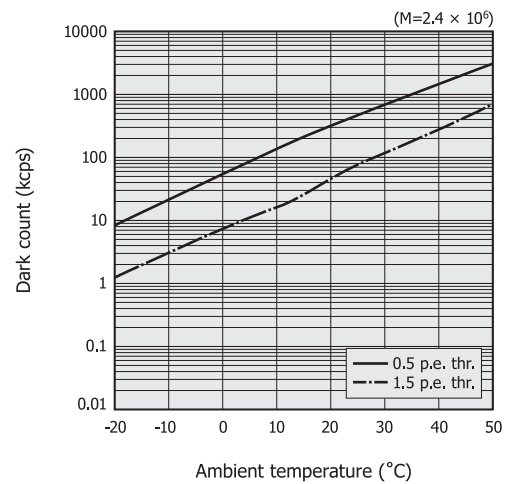
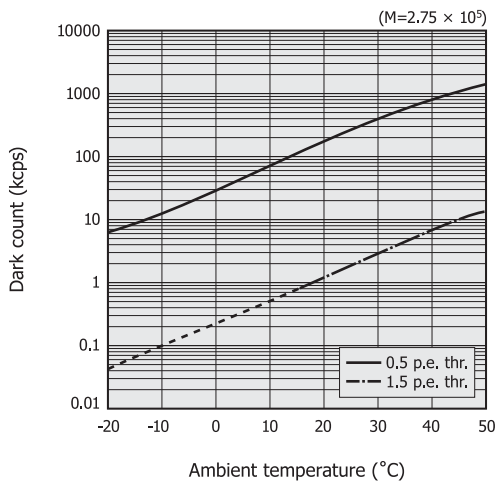
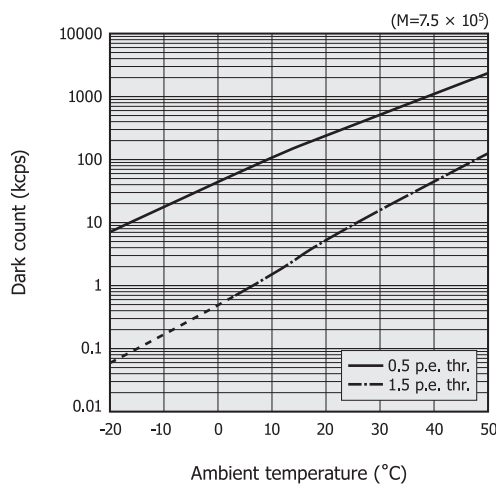


[Figure 3-12] Dark count vs. ambient temperature

(a) Active area: 1 mm sq, pixel size: 25 μm sq



(b) Active area: 1 mm sq, pixel size: 50 μm sq



3 - 5

Photon detection efficiency and dynamic range

Photon detection efficiency (PDE) is a measure of what percent of the incident photons is detected. Not all photons incident on an MPPC can be detected. Photon detection efficiency is expressed by equation (31). As the reverse voltage is increased, photon detection efficiency becomes higher, but this also causes an increase in the dark pulse, crosstalk, and afterpulse.

$$\text{PDE} = \text{QE} \times \text{Fg} \times \text{Pa} \dots\dots (31)$$

QE: quantum efficiency

Fg : fill factor $\left(= \frac{\text{Effective pixel size}}{\text{Pixel size}} \right)$

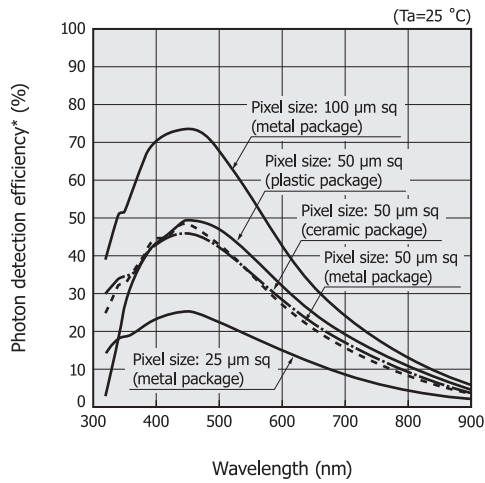
Pa : avalanche probability $\left(= \frac{\text{Number of excited pixels}}{\text{Number of photon-incident pixels}} \right)$

Since a quenching resistor is required for all pixels of an MPPC, the relative area the quenching resistors take up in the MPPC becomes larger as the number of pixels is increased. This means that the fill factor has a trade-off relation with the total number of pixels.

The MPPC has a peak photon detection efficiency at around 440 nm. This wavelength matches the emission wavelengths of scintillators such as LSO.

[Figure 3-13] Photon detection efficiency vs. wavelength (typical example)

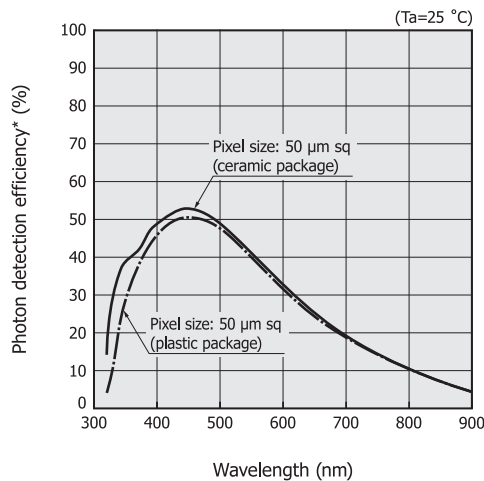
(a) Active area: 1 mm sq



* Photon detection efficiency includes effects of crosstalk and afterpulses.

KAPDB0130EB

(b) Active area: 3 mm sq



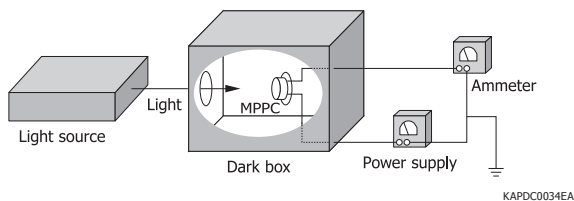
* Photon detection efficiency includes effects of crosstalk and afterpulses.

KAPDB0157EB

Photon detection efficiency measurement

This section describes how to calculate the photon detection efficiency from the MPPC output current using a monochromator.

[Figure 3-14] Connection example for photon detection efficiency measurement (using monochromator)



KAPDC0034EA

First, a photodiode with known spectral response characteristics is prepared. Based on its photo sensitivity at a given wavelength (ratio of photocurrent to incident light level, expressed in

A/W), the “number of photons incident on the photodiode” can be calculated from the photocurrent.

Next, the MPPC is installed in the same position as the photodiode, and the MPPC spectral response is then measured. The gain obtained when a reverse voltage is applied should already be known by checking it beforehand. By dividing the photocurrent obtained from the spectral response measurement by the charge (1.6×10^{-19} C) of an electron, the “number of photons detected by the MPPC” can be found.

The MPPC photon detection efficiency is then calculated by using equation (32):

$$\text{PDE} = \frac{\text{Number of photons detected by MPPC}}{\text{Number of photons incident on photodiode}} \times \frac{\text{Photodiode active area}}{\text{MPPC active area}} \dots (32)$$

Note: Since the number of photons detected by the MPPC is calculated from the photocurrent, the photon detection efficiency obtained by equation (32) also includes the effects from crosstalk and afterpulses.

Dynamic range

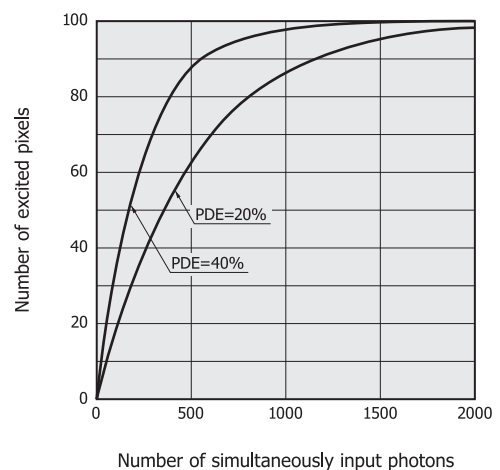
The total number of pixels and the photon detection efficiency of the MPPC determine the dynamic range for the simultaneously incident photons. Since each pixel only detects whether or not one or more photons have entered, the photon detection linearity lowers if the number of incident photons becomes large relative to the total number of pixels. This is because two or more photons begin to enter one pixel.

$$N_{\text{fired}} = N_{\text{total}} \times \left(1 - \exp \left(-\frac{N_{\text{photon}} \times \text{PDE}}{N_{\text{total}}} \right) \right) \dots (33)$$

N_{fired} : number of excited pixels
 N_{total} : total number of pixels
 N_{photon} : number of incident photons

Equation (33) shows that an MPPC with a larger number of pixels should be used to maintain output linearity versus an increase in the incident light level.

[Figure 3-15] Number of excited pixels vs. number of simultaneously input photons (theoretical values for 100-pixel MPPC)

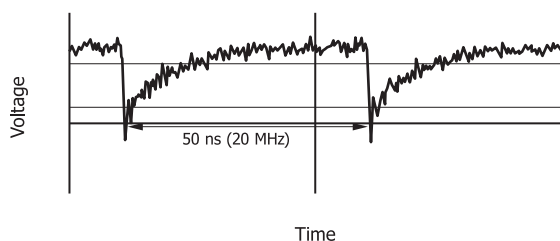


KAPDB0128EA

When a charge amplifier is used to measure the incident light having a certain time width, the substantial dynamic range widens. This is because, after a certain time period, the pixels which have produced pulses are restored to a state capable of detecting the next photons again. The time (recovery time) required for pixels to be restored 100% is approx. 20 ns for an MPPC with an active area of 1 mm sq and a pixel size of 25 μm sq, 50 ns for an MPPC with an active area of 1 mm sq and a pixel size of 50 μm sq, and 100 ns to 200 ns for an MPPC with an active area of 1 mm sq and a pixel size of 100 μm sq. Figure 3-16 shows an output measured when a photon enters a pixel of the MPPC with an active area of 1 mm sq and a pixel size of 50 μm sq, at a period nearly equal to the pulse length. It can be seen that the pulse is restored to a height equal to 100% of output.

[Figure 3-16] Pulse level recovery

(active area: 1 mm sq, pixel size: 50 μm sq)



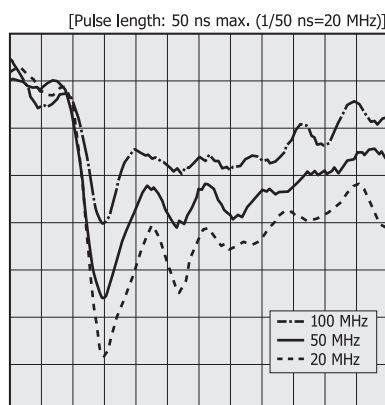
KAPDB0158EA

If the next input pulse enters before the output pulse is completely restored, then a small pulse is output, which does not reach the gain set by the operating voltage. In Figure 3-16, the rising region of the pulse indicates the process for charging the pixel. When the next photon is detected before the pixel is fully charged, the output pulse will have an amplitude that varies according to the charged level.

Figure 3-17 shows output pulse shapes obtained when light at different frequencies was input to a pixel.

[Figure 3-17] Output pulses obtained when light at different frequencies

was input (active area: 1 mm sq, pixel size: 50 μm sq)

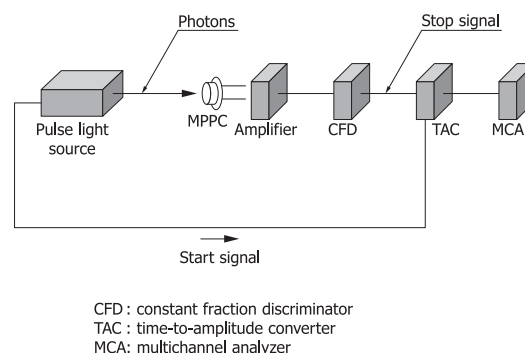


KAPDB0163EA

3-6 Time resolution

After light enters the MPPC active area, time is required for the multiplied pulse to appear as an output. The variation or jitter in this time determines the MPPC time resolution. As an example of measuring this jitter, the TTS (transit time spread) measurement method is described below.

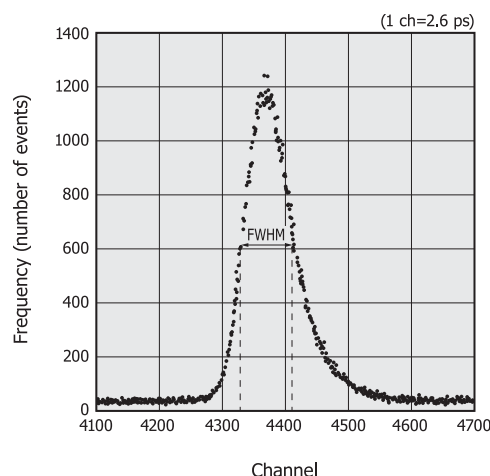
[Figure 3-18] Connection example



KAPDC0030EA

Figure 3-18 shows an example of connecting devices for TTS measurement. The pulse light source emits photons and simultaneously sends a start signal to the TAC. The TAC starts measuring the time upon receiving the start signal. Meanwhile, the photons enter the MPPC and the detected signals are amplified by the amplifier and sent to the CFD. When the CFD receives a signal with an amplitude exceeding the threshold for photon detection, it sends the signal to the TAC. The TAC receives the signal from the CFD as a stop signal for time measurement. At this point, the TAC also provides a pulse output proportional to the time from when photons entered the MPPC until the signal is output. The MCA analyzes the pulses received from the TAC and sorts them into different channels according to pulse height. The data stored in the MCA displays as a frequency distribution of MPPC responses.

[Figure 3-19] Pulse response distribution



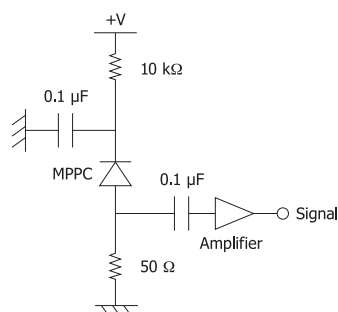
KAPDB0137EA

3-7 How to use

The MPPC characteristics change when the reverse voltage and ambient temperature are varied. For example, the gain, photon detection efficiency (PDE), and time resolution can be improved by increasing the reverse voltage. However, this is also accompanied by an increase in the dark count, crosstalk, and afterpulse. This trade-off in MPPC characteristics [Table 3-2] must be taken into account when setting the reverse voltage.

Figure 3-20 shows an example when connecting to a linear amplifier. A commonly used high-speed amplifier such as the HAMAMATSU C4890 for PIN photodiodes may be used as the linear amplifier.

[Figure 3-20] Connection example



KAPDC0024EA

Various methods can be used for photon counting with an MPPC. Three typical methods are described below.

Measuring pulses

The number of times a certain number of photons were simultaneously detected can be found by connecting an amp to an MPPC and measuring the output pulse heights.

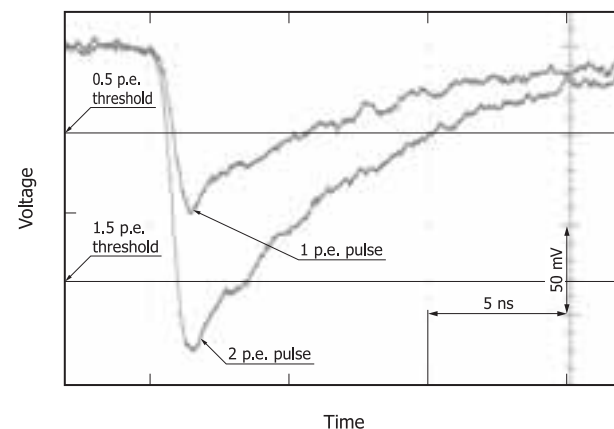
Before starting measurement, let a few photons enter the MPPC, and set the thresholds according to the number of photons so that pulses exceeding each threshold are counted on the frequency counter (electronic instrument for measuring the number of pulses exceeding a preset threshold).

(1) Counting the number of times that one or more photons are detected

Set the threshold at one-half (0.5 p.e.) the height of the “1 p.e.”

pulse [Figure 3-21]. Counting the number of pulses that exceed this threshold gives the number of times that one or more photons are detected.

[Figure 3-21] MPPC output waveform seen on oscilloscope



(2) Detecting two or more (or N or more) photons simultaneously

To count the number of times that two or more photons are detected simultaneously, set the threshold at the midpoint (1.5 p.e.) between “1 p.e.” and “2 p.e.” To count the number of times that N or more photons are simultaneously detected, set the threshold at a point of “N - 0.5 p.e.” Counting the number of pulses that exceed this threshold gives the number of times that N or more photons are simultaneously detected.

Measuring electric charge

The amount of the detected light can be estimated by using a charge amplifier, etc. to measure the electric charge that was output within a certain time period. This method is effective in measuring light that enters the MPPC with some temporal broadening but is not constant, such as when the MPPC is coupled to a scintillator. This method can measure the number of photons even if it exceeds the number of the MPPC pixels, as long as photons enter the MPPC at time intervals longer than the pixel recovery time.

Measuring output current

When measuring constant light, the number of photons can be estimated from the output current. If the number of incident photons per second is 1 Gcps ($=10^9$ cps) and measurement is

[Table 3-2] Characteristics that change with the reverse voltage and ambient temperature

Condition	Gain	Dark count	Crosstalk	Afterpulse	PDE	Time resolution
Increasing reverse voltage	□↗	□↗	□↗	□↗	□↗	□↗
Decreasing reverse voltage	□↘	□↘	□↘	□↘	□↘	□↘
Increasing ambient temperature (at constant gain)	-	□↗	-	□↘	-	-
Decreasing ambient temperature (at constant gain)	-	□↘	-	□↗	-	-

□↗: Increases

□↘: Decreases

- : Depends on conditions (or does not change)

performed with an MPPC whose gain is 7.5×10^5 , then the output current (I_s) is expressed by equation (34).

$$I_s = q \times (7.5 \times 10^5) \times 10^9 = 120 \mu\text{A} \dots\dots (34)$$

q : electron charge

If the dark count is 1 Mcps, the dark current (I_D) is given by equation (35).

$$I_D = q \times (7.5 \times 10^5) \times 10^6 = 120 \text{ nA} \dots\dots (35)$$

In this case, the dark current relative to the output current can be ignored. This method is effective when the amount of incident light is within the MPPC's dynamic range and also the output current is sufficiently larger than the dark current. Note that the output current contains crosstalk and afterpulse components.

■ Precautions for use (electrostatic measures)

Types with a pixel size of 100 μm sq are vulnerable to static electricity. If this might create problems, then take the following measures:

- Wear anti-static gloves when handling the sensors. Also wear anti-static clothing and a grounded wrist band to prevent damage by static electricity generated from friction, etc.
- Avoid directly placing the sensors on a workbench or floor where static charges might be present.
- Provide a ground connection to the workbench and floor to discharge static electricity.
- Electrically ground tools used to handle the sensors, such as tweezers and soldering irons.
- Install an appropriate protection circuit for the power supply, equipment, and measuring instrument according to the application, in order to prevent overvoltage and overcurrent damage.

3 - 8 New approaches

HAMAMATSU is making continuous improvements to extend the MPPC features such as compact size, low voltage operation, excellent time resolution, and immunity to magnetic fields.

The MPPC is promising for use with medical equipment such as PET scanners. For example, TOF-PET (time-of-flight - positron emission tomography) requires detectors with excellent time resolution to detect the positions of diseased parts with high accuracy. So we are further improving the MPPC time resolution to bring out its full potential.

Since the MPPC is unaffected by magnetic fields, its application is extending to astrophysics and elementary particle physics experiments to search for the origin of the universe and the root of matter. In the future, the MPPC may be utilized

for outer space applications. Detectors used in high energy accelerator experiments are subject to ever larger radiation dose. HAMAMATSU is currently at work developing MPPC that will be highly resistant to radiation damage.

The use of MPPC is also expected in analysis and measurement fields where low-level light is detected. In order to improve the MPPC photon-counting characteristics which are very important in these fields, HAMAMATSU is working to reduce dark components, crosstalk, and afterpulses; improve detection efficiency; and enhance sensitivity in the long wavelength region.

HAMAMATSU continues developing MPPC that will meet specific applications, opening new fields of MPPC application.

4. PSD (position sensitive detector)

Various methods are available for detecting the position of incident light, including methods using an array of many small detectors and a multi-element detector (such as CCD). In contrast to these, the PSD is a monolithic device designed to detect the position of incident light.

Since the PSD is a non-segmented photosensor that makes use of the surface resistance of the photodiode, it provides continuous electrical signals and offers excellent position resolution, fast response, and high reliability.

The PSD is used in a wide range of fields such as measurements of position, angles, distortion, vibration, and lens reflection/refraction. Applications also include precision measurement such as laser displacement meters, as well as optical remote control devices, distance sensors, and optical switches.

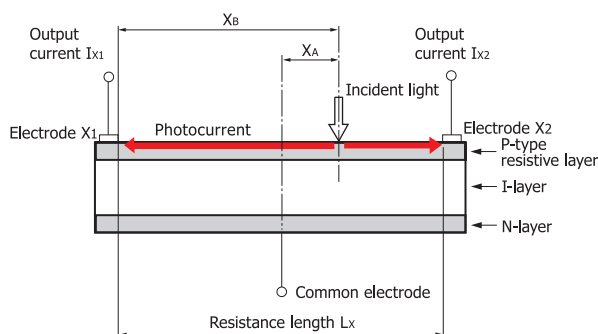
4-1 Features

- Excellent position resolution
- Wide spectral response range
- High-speed response
- Simultaneous detection of light level and center-of-gravity position of light spot
- High reliability

4-2 Structure and operating principle

A PSD basically consists of a uniform resistive layer formed on one or both surfaces of a high-resistivity semiconductor substrate and a pair of electrodes formed on both ends of the resistive layer for extracting position signals. The active area, which is also a resistive layer, has a PN junction that generates photocurrent by means of the photovoltaic effect.

[Figure 4-1] Schematic of PSD cross section



KP5DC0005EA

Figure 4-1 is a schematic view of a PSD cross section showing the operating principle. Above an N-type high-resistivity silicon substrate, a P-type resistive layer is formed that serves as an active area for photoelectric conversion and a resistive layer. A pair of output electrodes is formed on both ends of the P-type resistive layer. The backside of the silicon substrate is an N-layer to which a common electrode is connected. Basically, this is the same structure as that of PIN photodiodes except for the P-type resistive layer on the surface.

When a light spot strikes the PSD, an electric charge proportional to the light level is generated at the light incident position. This electric charge flows as photocurrents through the resistive layer and is extracted from the output electrodes X1 and X2, while being divided in inverse proportion to the distance between the light incident position and each electrode. In Figure 4-1, the relation between the incident light position and the photocurrents from the output electrodes X1 and X2 is as follows:

- When the center point of the PSD is set as the origin:

$$I_{X1} = \frac{\frac{L_X}{2} - X_A}{L_X} \times I_o \quad \dots\dots (36) \quad I_{X2} = \frac{\frac{L_X}{2} + X_A}{L_X} \times I_o \quad \dots\dots (37)$$

$$\frac{I_{X2} - I_{X1}}{I_{X1} + I_{X2}} = \frac{2X_A}{L_X} \quad \dots\dots (38) \quad \frac{I_{X1}}{I_{X2}} = \frac{L_X - 2X_A}{L_X + 2X_A} \quad \dots\dots (39)$$

- When the end of the PSD is set as the origin:

$$I_{X1} = \frac{L_X - X_B}{L_X} \times I_o \quad \dots\dots (40) \quad I_{X2} = \frac{X_B}{L_X} \times I_o \quad \dots\dots (41)$$

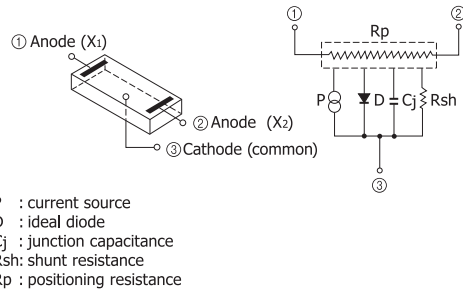
$$\frac{I_{X2} - I_{X1}}{I_{X1} + I_{X2}} = \frac{2X_B - L_X}{L_X} \quad \dots\dots (42) \quad \frac{I_{X1}}{I_{X2}} = \frac{L_X - X_B}{X_B} \quad \dots\dots (43)$$

IX1: output current from electrode X1
IX2: output current from electrode X2
Io : total photocurrent (IX1 + IX2)
LX : resistance length (length of active area)
XA : distance from electrical center of PSD to light incident position
XB : distance from electrode X1 to light incident position

By finding the values of IX1 and IX2 from equations (36) and (37) or (40) and (41) and placing them in equations (38) and (39) or (42) and (43), the light incident position can be obtained irrespective of the incident light level and its changes. The light incident position obtained here corresponds to the center-of-gravity of the light spot.

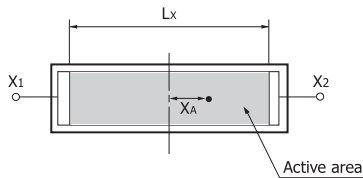
One-dimensional PSD

[Figure 4-2] Structure and equivalent circuit (one-dimensional PSD)



KPSDC0006EA

[Figure 4-3] Active area (one-dimensional PSD)



KPSDC0010EB

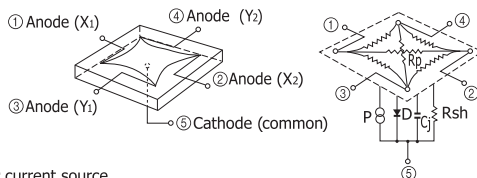
● Incident position conversion formula (See also Figure 4-3.)

$$\frac{I_{X2} - I_{X1}}{I_{X1} + I_{X2}} = \frac{2X_A}{L_x} \dots\dots\dots (44)$$

Two-dimensional PSD

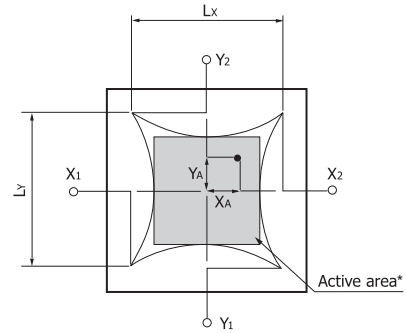
The shapes of the active area and electrodes of two-dimensional PSDs have been improved to suppress interactions between the electrodes. Besides the advantages of small dark current, high-speed response, and easy application of reverse voltage, the circumference distortion has been greatly reduced. The light incident position is calculated using the incident position conversion formulas which are shown in equations (45) and (46).

[Figure 4-4] Structure and equivalent circuit (two-dimensional PSD)



KPSDC0009EB

[Figure 4-5] Active area (two-dimensional PSD)



* Active area is specified as the inscribed square.

KPSDC0012EC

● Incident position conversion formulas (See also Figure 4-5.)

$$\frac{(I_{X2} + I_{Y1}) - (I_{X1} + I_{Y2})}{I_{X1} + I_{X2} + I_{Y1} + I_{Y2}} = \frac{2X_A}{L_x} \dots\dots\dots (45) \quad \square e$$

$$\frac{(I_{X2} + I_{Y2}) - (I_{X1} + I_{Y1})}{I_{X1} + I_{X2} + I_{Y1} + I_{Y2}} = \frac{2Y_A}{L_y} \dots\dots\dots (46)$$

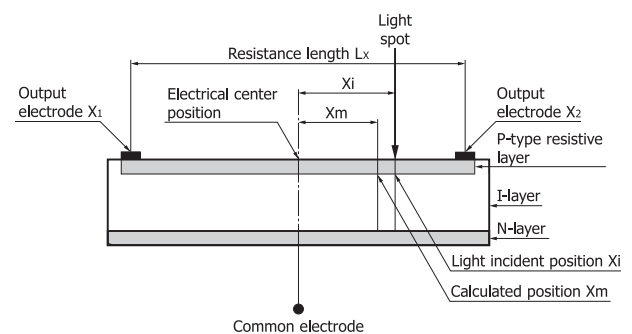
4-3 Position detection error

The position of a light spot incident on the PSD surface can be measured by making calculations based on the photocurrent extracted from each output electrode. The position obtained with the PSD is the center-of-gravity of the light spot, and it is independent of the light spot size, shape, and intensity.

However, the calculated position usually varies slightly in each PSD from the actual position of the incident light. This difference is referred to as the “position detection error” and is one of the most important characteristics of a PSD.

If a light spot strikes the PSD surface and the photocurrents extracted from the output electrodes are equal, the position of the incident light spot on the PSD is viewed as the electrical center position. Using this electrical center position as the origin point, the position detection error is defined as the difference between the position at which the light is actually incident on the PSD and the position calculated from the PSD photocurrents.

[Figure 4-6] Schematic of PSD cross section



KPSDC0071EB

A position detection error is calculated as described below. In Figure 4-6, which shows the electrical center position as the reference position (origin point), if the actual position of incident light is X_i , the photocurrents obtained at the output electrodes are I_{x1} and I_{x2} , and the position calculated from the photocurrents is X_m , then the difference in distance between X_i and X_m is defined as the position detection error (E).

$$E = X_i - X_m \text{ [}\mu\text{m]} \quad (47)$$

X_i : actual position of incident light [μm]
 X_m : calculated position [μm]

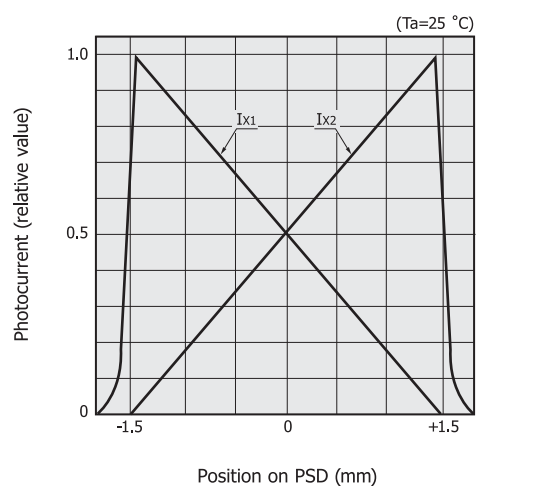
$$X_m = \frac{I_{x2} - I_{x1}}{I_{x1} + I_{x2}} \times \frac{L_x}{2} \quad (48)$$

The position detection error is measured under the following conditions.

- Light source : $\lambda=830 \text{ nm}$
- Light spot size : $\phi 200 \mu\text{m}$
- Total photocurrent : $10 \mu\text{A}$
- Reverse voltage : specified value listed in our datasheets

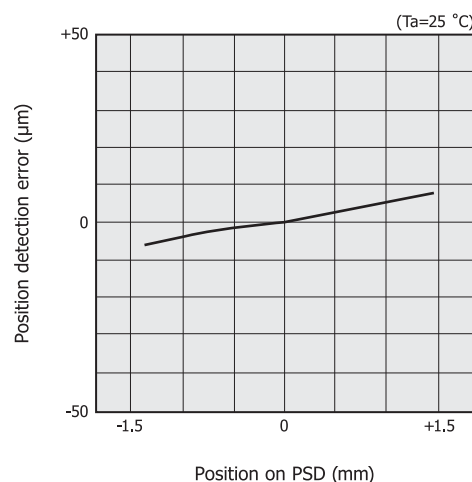
Figure 4-7 shows the photocurrent output example from each electrode of a one-dimensional PSD with a resistance length of 3 mm (S4583-04, etc.). The position detection error estimated from the obtained data is also shown in Figure 4-8.

[Figure 4-7] Photocurrent output example of one-dimensional PSD (S4583-04, etc.)



KPSDB0114EA

[Figure 4-8] Position detection error example of one-dimensional PSD (S4583-04, etc.)

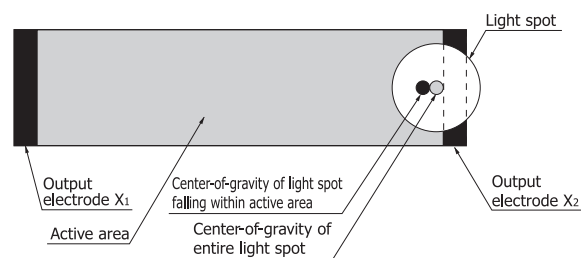


KPSDB0005EA

Specified area for position detection error

The light spot position can be detected over the entire active area of a PSD. However, if part of the light spot strikes outside the PSD active area, a positional shift in the center-of-gravity occurs between the entire light spot and the light spot falling within the active area, making the position measurement unreliable. It is therefore necessary to select a PSD whose active area matches the incident light spot.

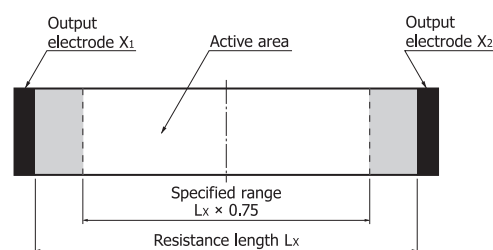
[Figure 4-9] Center-of-gravity of incident light spot



KPSDC0073EA

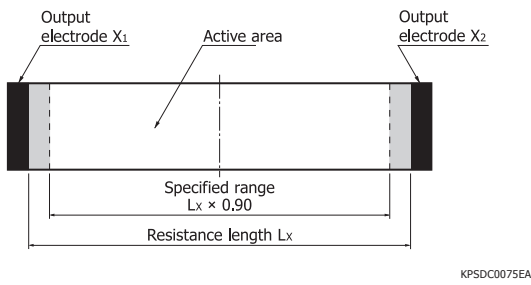
The areas used to measure position detection errors are specified as shown in Figure 4-10.

[Figure 4-10] Specified range for position detection error
(a) One-dimensional PSD (resistance length $\leq 12 \text{ mm}$)

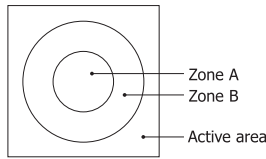


KPSDC0074EA

(b) One-dimensional PSD (resistance length > 12 mm)



(c) Two-dimensional PSD



Zone A: Within a circle with a diameter equal to 40% of one side length of the active area
Zone B: Within a circle with a diameter equal to 80% of one side length of the active area

On two-dimensional PSDs, the position detection error along the circumference is larger than that in the center of the active area, so the error is specified separately in Zone A and Zone B.

4-4 Position resolution

Position resolution is defined as the minimum detectable displacement of a light spot incident on a PSD, and it is expressed as a distance on the PSD active area. Position resolution is determined by the PSD resistance length and the S/N. Using equation (41) for position calculation as an example, equation (49) can be established.

$$Ix2 + \Delta I = \frac{XB + \Delta X}{Lx} \times Io \dots\dots\dots (49)$$

ΔI : change in output current
 ΔX : small displacement of light spot

Then, Δx can be expressed by equation (50).

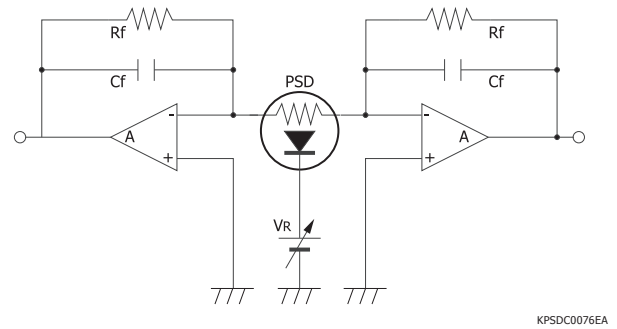
$$\Delta x = Lx \times \frac{\Delta I}{Io} \dots\dots\dots (50)$$

When the positional change is infinitely small, the noise component contained in the output current $Ix2$ determines the position resolution. If the PSD noise current is In , then the position resolution (ΔR) is generally expressed by equation (51).

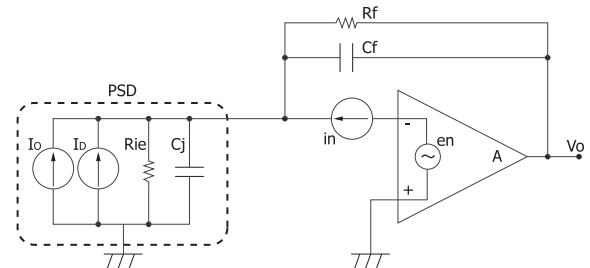
$$\Delta R = Lx \times \frac{In}{Io} \dots\dots\dots (51)$$

Figure 4-11 shows the connection example when using a one-dimensional PSD with current-to-voltage conversion op amps. The noise model for this circuit is shown in Figure 4-12.

[Figure 4-11] Connection example of one-dimensional PSD and current-to-voltage conversion op amps



[Figure 4-12] Noise model



Io : photocurrent
 Id : dark current
 Rie : interelectrode resistance
 Cj : junction capacitance
 Rf : feedback resistance
 Cf : feedback capacitance
 in : equivalent input current noise of op amp
 en : equivalent input voltage noise of op amp
 Vo : output voltage

Noise current

Noise currents that determine the position resolution are described below.

(1) When $Rf \gg Rie$

If the feedback resistance (Rf) of the current-to-voltage converter circuit is sufficiently greater than the PSD interelectrode resistance (Rie), the noise current is calculated using equation (54). In this case, $1/Rf$ can be ignored since it is sufficiently small compared to $1/Rie$.

- Shot noise current Is originating from photocurrent and dark current

$$Is = \sqrt{2q \times (Io + Id) \times B} \text{ [A]} \dots\dots\dots (52)$$

q : electron charge [C]
 Io : photocurrent [A]
 Id : dark current [A]
 B : bandwidth [Hz]

- Thermal noise current (Johnson noise current) I_j generated from interelectrode resistance

$$I_j = \sqrt{\frac{4kTB}{R_{ie}}} \text{ [A]} \dots\dots\dots (53)$$

k : Boltzmann's constant [J/K]
T : absolute temperature [K]
R_{ie}: interelectrode resistance [Ω]

Note: R_{sh} can be usually ignored as R_{sh} >> R_{ie}.

- Noise current I_{en} by op amp equivalent input voltage noise

$$I_{en} = \frac{e_n}{R_{ie}} \sqrt{B} \text{ [A]} \dots\dots\dots (54)$$

e_n: equivalent input voltage noise of op amp [V/Hz^{1/2}]

By taking the sum of equations (52), (53), and (54), the PSD noise current (I_n) can be expressed as an effective value (rms) by equation (55).

$$I_n = \sqrt{I_s^2 + I_j^2 + I_{en}^2} \text{ [A]} \dots\dots\dots (55)$$

(2) If R_f cannot be ignored versus R_{ie}
(when R_{ie}/R_f is larger than about 0.1)

The noise current is calculated by converting it to an output noise voltage. In this case, equations (52), (53), and (54) are respectively converted into output voltages as follows:

$$V_s = R_f \times \sqrt{2q \times (I_o + I_D) \times B} \text{ [V]} \dots\dots\dots (56)$$

$$V_j = R_f \times \sqrt{\frac{4kTB}{R_{ie}}} \text{ [V]} \dots\dots\dots (57)$$

$$V_{en} = \left(1 + \frac{R_f}{R_{ie}}\right) \times e_n \times \sqrt{B} \text{ [V]} \dots\dots\dots (58)$$

The thermal noise from the feedback resistance and the op amp equivalent input current noise are also added as follows:

- Thermal noise voltage V_{Rf} generated by feedback resistance

$$V_{Rf} = R_f \times \sqrt{\frac{4kTB}{R_f}} \text{ [V]} \dots\dots\dots (59)$$

- Op amp equivalent input voltage noise V_{in}

$$V_{in} = R_f \times i_n \times \sqrt{B} \text{ [V]} \dots\dots\dots (60)$$

i_n: op amp equivalent input current noise [A/Hz^{1/2}]

The op amp output voltage noise (V_n) is then expressed as an effective value (rms) by equation (61).

$$V_n = \sqrt{V_s^2 + V_j^2 + V_{en}^2 + V_{Rf}^2 + V_{in}^2} \text{ [V]} \dots\dots\dots (61)$$

Figure 4-13 shows the shot noise current plotted versus the photocurrent value when R_f >> R_{ie}. Figure 4-14 shows the thermal noise and the noise current by the op amp equivalent input voltage noise plotted versus the interelectrode resistance value. When using a PSD with an interelectrode resistance of about 10 kΩ, the op amp characteristics become a crucial

factor in determining the noise current, so a low-noise current op amp must be used. When using a PSD with an interelectrode resistance exceeding 100 kΩ, the thermal noise generated from the interelectrode resistance of the PSD itself will be predominant.

[Figure 4-13] Shot noise current vs. photocurrent

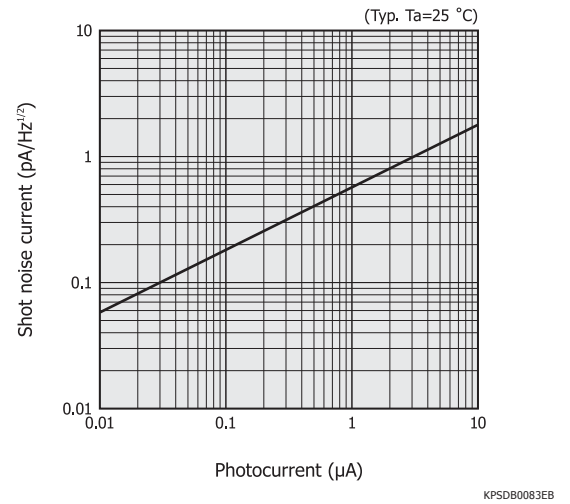
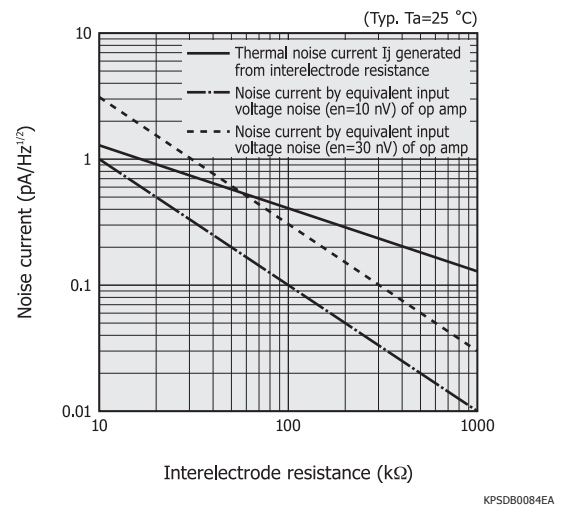


[Figure 4-14] Noise current vs. interelectrode resistance



As explained, the position resolution of a PSD is determined by the interelectrode resistance and photocurrent. This is the point in which the PSD greatly differs from segmented type position detectors. The following methods are effective for improving the PSD position resolution.

- Increase the signal photocurrent (I_o).
- Increase the interelectrode resistance (R_{ie}).
- Shorten the resistance length (L_x).
- Use an op amp with appropriate noise characteristics.

HAMAMATSU measures and calculates the position resolution under the conditions that the photocurrent is 1 μA, the circuit input noise is 1 μV (31.6 nV/Hz^{1/2}), and the frequency

bandwidth is 1 kHz.

4-5 Response speed

As with photodiodes, the response speed of a PSD is the time required for the generated carriers to be extracted as current to an external circuit. This is generally expressed as the rise time and is an important parameter when detecting a light spot moving on the active surface at high speeds or when using a signal light source driven by pulse for background light subtraction. The rise time is defined as the time needed for the output signal to rise from 10% to 90% of its peak and is mainly determined by the following two factors:

(1) Time constant t_1 determined by the interelectrode resistance, load resistance, and terminal capacitance

The interelectrode resistance (R_{ie}) of a PSD basically acts as load resistance (R_L), so the time constant t_1 determined by the interelectrode resistance and terminal capacitance (C_t) is expressed as in equation (62).

$$t_1 = 2.2 \times C_t \times (R_{ie} + R_L) \dots\dots\dots (62)$$

The interelectrode resistance of a PSD is distributed between the electrodes. HAMAMATSU measures the response speed with a light spot incident on the center of the active area, so equation (62) roughly becomes equation (63).

$$t_1 = 0.5 \times C_t \times (R_{ie} + R_L) \dots\dots\dots (63)$$

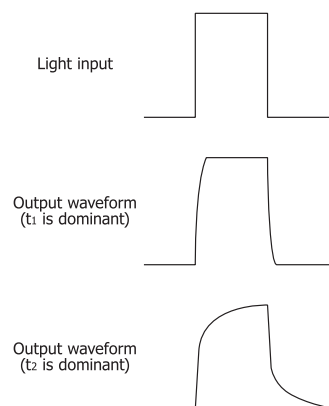
(2) Diffusion time t_2 of carriers generated outside the depletion layer

Carriers are also generated outside the depletion layer when light enters the PSD chip peripheral areas outside the active area or when light is absorbed at locations deeper than the depletion layer in the substrate. These carriers diffuse through the substrate and are extracted as an output. The time t_2 required for these carriers to diffuse may be more than several microseconds.

Equation (64) gives the approximate rise time (t_r) of a PSD, and Figure 4-15 shows output waveform examples in response to light input.

$$t_r \approx \sqrt{t_1^2 + t_2^2} \dots\dots\dots (64)$$

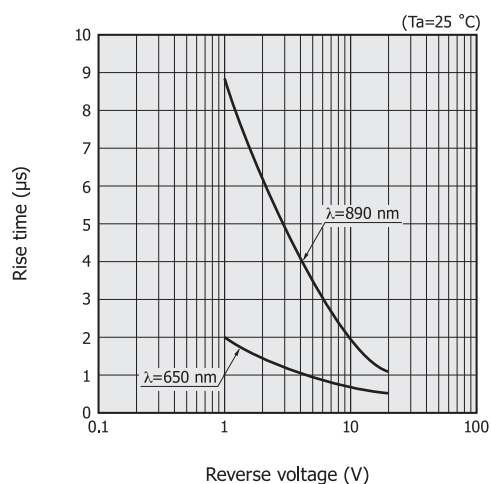
[Figure 4-15] Example of PSD response waveforms



KPSDC0078EA

Figure 4-16 shows the relation between the rise time and reverse voltage measured at different wavelengths. As seen from the figure, the rise time can be shortened by using light of shorter wavelengths and increasing the reverse voltage. Selecting a PSD with a small interelectrode resistance is also effective in improving the rise time.

[Figure 4-16] Rise time vs. reverse voltage (typical example)



KPSDB0110EB

4-6 Saturation photocurrent

Photocurrent saturation must be taken into account when a PSD is used in locations such as outdoors where the background light level is high, or when the signal light level is extremely large. Figure 4-17 shows an output example of a non-saturated PSD. This PSD is operating normally with good output linearity over the entire active area.

Figure 4-18 shows an output example of a saturated PSD. This PSD does not function correctly since the output linearity is lost.

Photocurrent saturation of a PSD depends on the interelectrode resistance and reverse voltage [Figure 4-19]. The saturation photocurrent is specified as the total photocurrent measurable when the entire active area is illuminated. If a small light spot is focused on the active area, the photocurrent will be

concentrated only on a localized portion, so saturation will occur at a lower level than specified.

To avoid the saturation effect, use the following methods.

- Reduce the background light level by using an optical filter.
- Use a PSD with a small active area.
- Increase the reverse voltage.
- Decrease the interelectrode resistance.
- Make the light spot larger than a certain size.

[Figure 4-17] Photocurrent output example of PSD in normal operation (S5629)

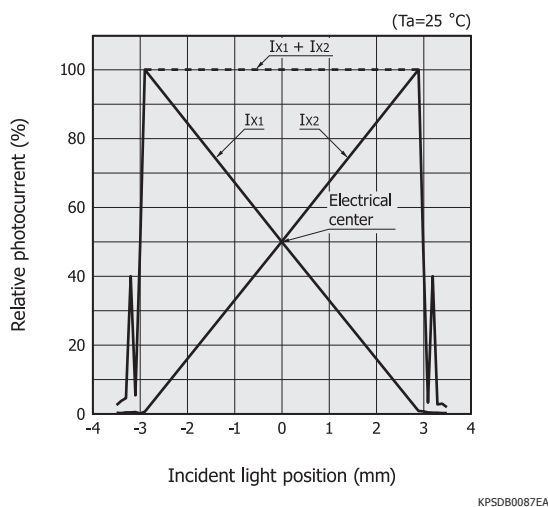


[Figure 4-18] Photocurrent output example of saturated PSD (S5629)

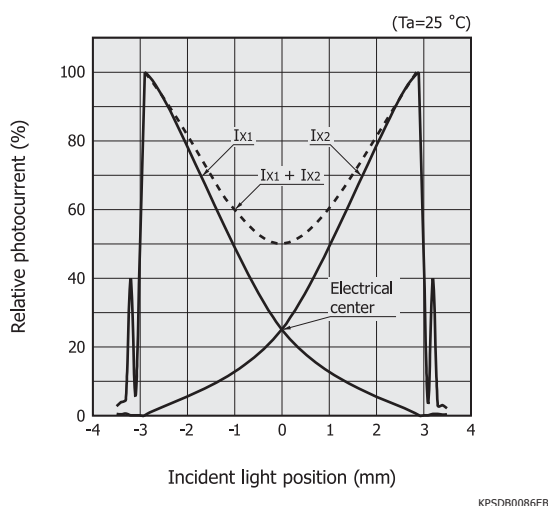
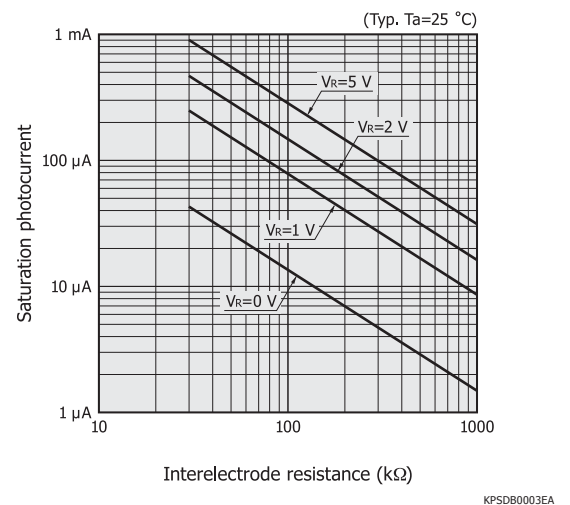


[Figure 4-19] Saturation photocurrent vs. interelectrode resistance (entire active area fully illuminated)



4 - 7 How to use

Recommended circuits

(1) Operating circuit examples

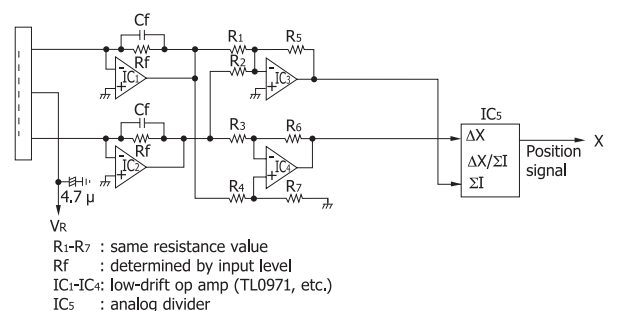
The output of a PSD is current, which is usually converted to a voltage signal using an op amp and then arithmetically processed with a dedicated IC. Typical circuits are shown in Figures 4-20 and 4-21. The calculated position output does not change even if the light level fluctuates due to changes in the distance between the PSD and the light source or in the light source brightness.

If background light exists, use a pulse-driven light source to eliminate the photocurrent caused by background light, and only AC signal components should be extracted by AC-coupling the PSD to current-to-voltage conversion amps like the circuit shown in Figure 4-21.

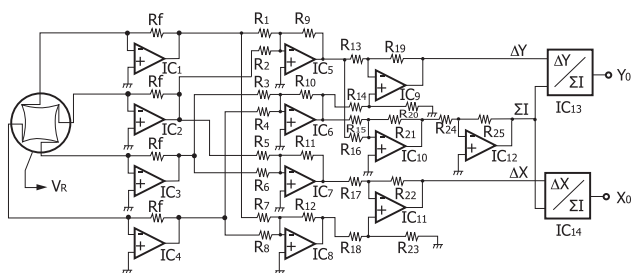
Figure 4-22 shows the block diagram of an operating circuit with a digital output that allows data transfer to a PC. This circuit arithmetically processes the PSD output current with the microcontroller after performing current-to-voltage conversion and A/D conversion.

[Figure 4-20] DC-operating circuit examples

(a) For one-dimensional PSD



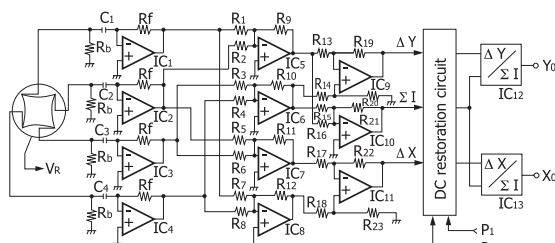
(b) For two-dimensional PSD



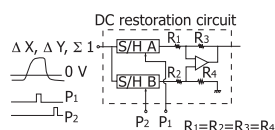
R1-R25 : same resistance value
Rf : determined by input level
IC1-IC12 : low-drift op amp (TL0971, etc.)
IC13, IC14: analog divider

KPSDC0026EE

[Figure 4-21] AC-operating circuit example
(for two-dimensional PSD)

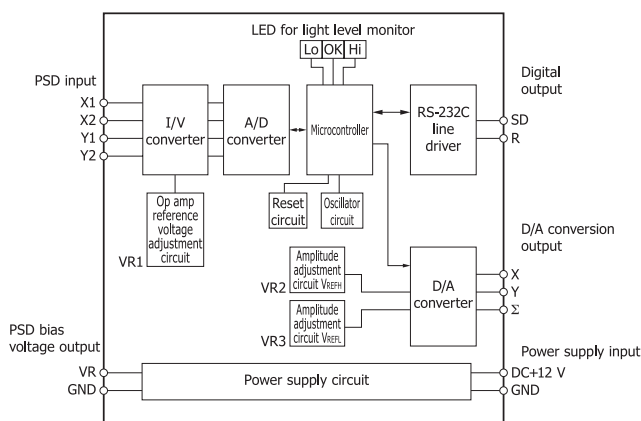


R1-R24 : same resistance value
Rf : determined by input level
IC1-IC11 : low-drift op amp (TL0971, etc.)
IC12, IC13: analog divider



KPSDC0029EE

[Figure 4-22] Block diagram of DC-operating circuit with digital output (C9069)



KACCC0223EA

(2) PSD signal processing circuits

[Figure 4-23] Two-dimensional PSD signal processing circuit
C9069



HAMAMATSU provides various types of PSD signal processing circuits to help users easily evaluate one-dimensional and two-dimensional PSDs. These include a DC signal processing circuit assembled on a compact board that contains a current-to-voltage converter circuit, addition/subtraction circuit, and analog divider circuit similar to the DC-operating circuit examples described above. Also available is an AC signal processing circuit that contains a sync circuit and LED drive circuit in addition to the AC-operating circuit example described above, so measurement can be started by simply connecting to a power supply (± 15 V) and an LED.

HAMAMATSU also offers a digital-output signal processing circuit that uses a microcontroller to perform all position calculations such as addition/subtraction and division. Stable position output can be obtained in measurements where the light level is high but brightness changes are small. This processing circuit is easy to handle as it operates on an AC power adapter.

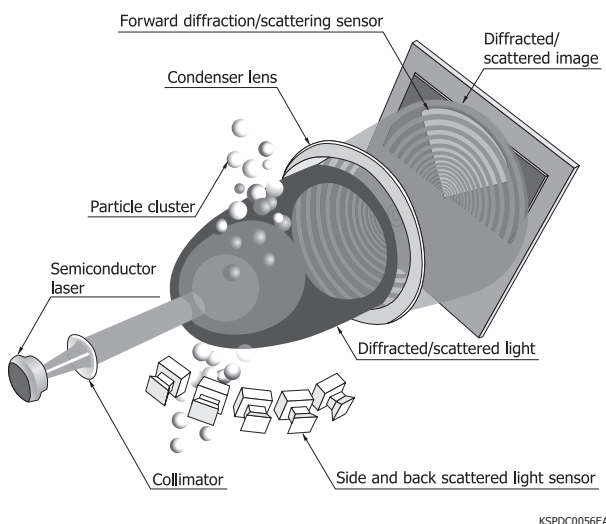
5. Applications

5-1 Particle size analyzers (laser diffraction/scattering method)

The laser diffraction and scattering method is a particle size measurement technique offering features such as a short measurement time, good reproduction, and measurement of the particle flow state. Irradiating a laser beam (monochrome collimated beam) onto the particles for measurement generates a light level distribution pattern from spatially diffracted and scattered light. This distribution pattern changes with the size of the particles. Large area sensors with high resolution are needed to detect the diffracted and scattered light.

HAMAMATSU multi-element Si photodiodes have superb sensitivity and small characteristic variations between elements. These photodiodes are manufactured using our sophisticated “large chip mounting/processing” technology. Many of them are used in sensor units (forward diffracted/scattered light sensors & side and back scattered light sensors) which are the core of the particle size analyzers. These photodiodes are also incorporated in particle size analyzers capable of measuring particles from 0.015 μm to 3 mm, and so are used for environmental measurements.

[Figure 5-1] Schematic of particle size distribution analyzer (laser diffraction and scattering method)



5-2 Barcode readers

A barcode reader consists of a light source, a lens, and a photosensor. The light source such as an LED or laser diode emits light onto the barcode surface, and the lens focuses the light reflected from that surface, which is then detected by the photosensor. The detected pattern is compared with the registered patterns and then decoded into characters and

numbers.

The photosensor in the barcode reader must have high-speed response and high sensitivity, and it must also be able to detect the reflected light accurately. HAMAMATSU Si PIN photodiodes meet all these needs, and their photosensitive surface has small variations in sensitivity and so can detect light with high stability at any position on the photosensitive surface. HAMAMATSU also offers advanced technology for filter mounting to block extraneous light and for precision mounting and micro-assembly, which will help make the barcode readers smaller in size.

5-3 UV sensors

Ultraviolet rays are high energy light and have sterilizing effects and photocatalytic reactions. On the other hand, ultraviolet rays deteriorate the materials that absorb them.

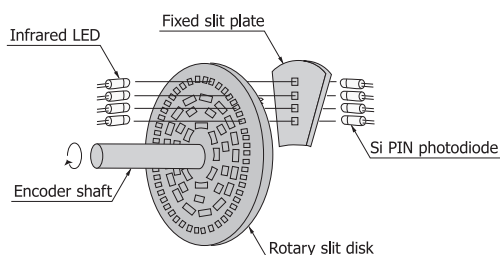
Si photodiodes also have sensitivity in the ultraviolet region and so are widely used for detecting ultraviolet light. Ordinary Si photodiodes have the problem that ultraviolet light reacts with resin which causes outgassing (slow release of gas from material) that might lower sensitivity. HAMAMATSU Si photodiodes do not use such resin materials to bond the chips and seal the windows. We have also developed Si photodiode chips highly resistant to ultraviolet light, so they can be used to design high-sensitivity and high-reliability UV sensors. We also supply Si photodiodes that are hermetically sealed in high-reliability packages along with monochromatic band-pass filters, and these are widely used in equipment for detecting organic contamination which is one cause of water pollution.

5-4 Rotary encoders

Rotary encoders are widely used in FA (factory automation) and industrial control equipment, etc. Rotary encoders contain a rotary slit disk and fixed slit plate between a light emitter and a photosensor (photodiode). The rotation of the rotary slit disk serves to pass or block light from the light emitter, and changes in this light are detected by the photosensor as rotations.

The photosensor must have high-speed response and high chip position accuracy in order to convert the number of shaft rotations (analog values) into pulses (digital values). Multi-element Si PIN photodiodes made by HAMAMATSU are suitable for detecting high-speed changes in the optical signal. These photosensors deliver stable detection because there is small variation in sensitivity and response speed between elements. To ensure low photosensor noise, patterning technology may be applied to block light to sections other than the photosensitive areas.

[Figure 5-2] Example of rotary encoder structure



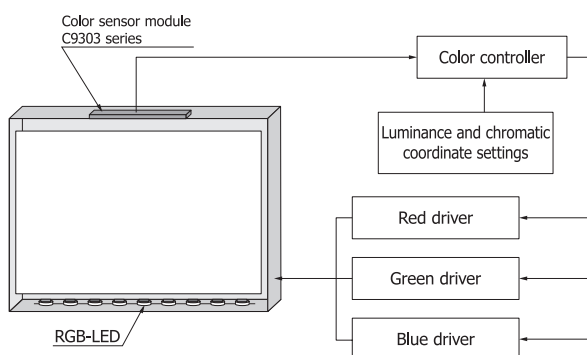
KSPDC0062EA

5-5 Color sensors

Separately detecting the three primary colors of light, which are red (R), green (G), and blue (B) color signals, not only simplifies color identification but also makes it possible to authenticate paper money, identify paint colors, and manage printed matter and textile product colors, etc. Si photodiodes have sensitivity over a wide wavelength range. However, combining them with filters allows detecting the individual RGB wavelengths. HAMAMATSU Si photodiodes for color sensors are small since each of the RGB sensors is integrated on the same chip and allows easy detection of color signals.

In recent years, attention is paid to TFT liquid crystal backlighting using RGB-LED because of its mercury-free design and good color reproduction. Color sensor modules using HAMAMATSU Si photodiodes are used to detect each color of RGB-LED in order to compensate for color changes caused by RGB-LED temperature characteristics and deterioration.

[Figure 5-3] Color adjustment in TFT liquid crystal backlighting using RGB-LED (application example of C9303 series)



LED: made by Lumileds (LUXEON), <http://www.lumileds.com/>
Color controller: made by Delta, <http://www.deltaww.com/>

KACCC0212ED

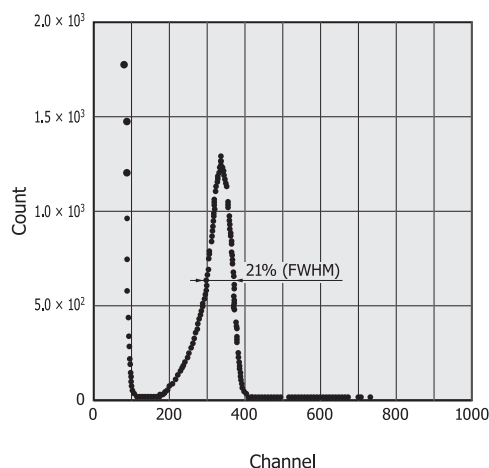
[Figure 5-4] Color sensor module C9303 series



5-6 X-ray detection

As with Si PIN photodiodes, Si APDs are also used for direct X-ray detection. Since Si APDs internally multiply the signal, they can measure lower energy radiation at higher speeds compared to Si PIN photodiodes.

[Figure 5-5] Energy spectrum measurement example (Si APD S8890 series, $E=16.53$ keV)



KAPDB0093EA

Reference

"A fast detector using stacked avalanche photodiodes for x-ray diffraction experiments with synchrotron radiation." Review of Scientific Instruments Vol. 69 No. 2, Part 1, Feb. 1998, S. Kishimoto, N. Ishizawa, T. P. Vaalsta

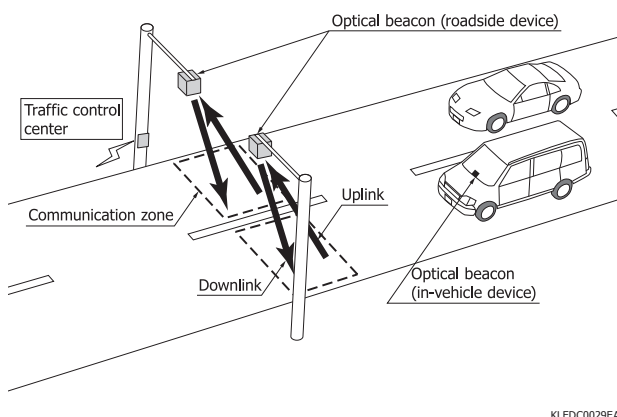
5-7 VICS (Vehicle Information and Communication System)

VICS is a system used in Japan for providing information such as traffic congestion, road construction, traffic regulations, and required time, etc. by media such as FM multiplex broadcasts, radio waves, and light.

Information supplied by light (optical media) makes use of optical beacons (in-vehicle devices) mounted in the vehicle and optical beacons (roadside devices) mounted at major

points on the road to carry out two-way communication by near infrared light. One advantage of this method is that unlike other communication media, information can be exchanged in both directions. A disadvantage however is that only pinpoint information can be provided since the communication area is limited. The uplink (in-vehicle device → roadside device) communication range is different from the downlink (roadside device → in-vehicle device) range.

[Figure 5-6] Optical beacons used by VICS



The optical beacon contains an LED and a photodiode. The in-vehicle device must be compact to avoid installation space problems and uses a surface mount type photodiode. The in-vehicle device will have to operate under harsh environmental conditions, so the design specifications must allow for a wider operating and storage temperature range than in ordinary photodiodes.

In early-stage VICS systems, the LED array and the photodiode were almost always mounted separately. Currently, however, both are integrated into one compact device [Figure 5-7].

[Figure 5-7] Light emitting/receiving module P8212 for VICS



5-8 Medical equipment and high energy physics experiments

In the medical equipment field, the MPPC is a promising device for applications such as high-resolution PET (positron emission tomography) and TOF (time-of-flight) PET.

In MRI-PET scanning where the MRI generates an extremely

strong magnetic field, the MPPC is suitable for PET detectors because it is unaffected by magnetic fields.

The MPPC is also a promising candidate for high-energy accelerator experiments to discover the ultimate constituents of matter. The European Organization for Nuclear Research (called CERN) is presently assessing the MPPC for use in calorimeter units needed to detect particle energy in its next-generation International Linear Collider (ILC). Moreover, in Japan, the High Energy Accelerator Research Organization (KEK) and the Japan Atomic Energy Agency (JAEA) are planning a joint experiment at the Japan Proton Accelerator Research Complex (called J-PARC) being built in Tokai-mura (Ibaraki Prefecture). This experiment called "T2K" (Tokai to Kamioka) will verify whether or not the neutrino has mass, by sending neutrino beams to Super-Kamiokande (Gifu Prefecture, about 300 km away from Tokai-mura). A large number of MPPC (62000 pieces) are scheduled for use in monitoring the neutrino beams in this experiment.

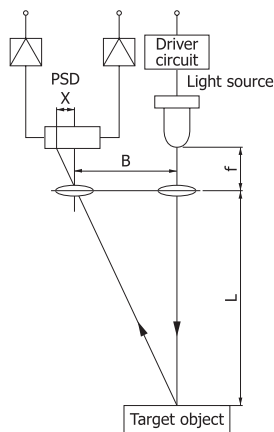
References

- IEEE, "2006 Nuclear Science Symposium" record CD-ROM
- 1 "Development of Multi-Pixel Photon Counters"
 - S. Gomi, M. Taguchi, H. Hano, S. Itoh, T. Kubota, T. Maeda, Y. Mazuka, H. Otono, E. Sano, Y. Sudo, T. Tsubokawa, M. Yamaoka, H. Yamazaki, S. Uozumi, T. Yoshioka, T. Iijima, K. Kawagoe, S. H. Kim, T. Matsumura, K. Miyabayashi, T. Murakami, T. Nakadaira, T. Nakaya, T. Shinkawa, T. Takeshita, M. Yokoyama, and K. Yoshimura
- 2 "Development of Multi-Pixel Photon Counter (MPPC)"
 - K. Yamamoto, K. Yamamura, K. Sato, T. Ota, H. Suzuki, and S. Ohsuka
- © IEEE, 2006 Nuclear Science Symposium, 29th Oct. to 4th Nov., 2006, San Diego, California
- IEEE, "2007 Nuclear Science Symposium" record CD-ROM
- "Development of Multi-Pixel Photon Counter (MPPC)"
 - K. Yamamoto, K. Yamamura, K. Sato, S. Kamakura, T. Ota, H. Suzuki, S. Ohsuka
- © IEEE, 2007 Nuclear Science Symposium, 27th Oct. to 3th Nov., 2007, Honolulu, Hawaii
- <http://www-conf.kek.jp/PD07/>
- International workshop on new photon-detectors PD07, 27th Jun. to 29th Jun. 2007 Kobe, Japan

5-9 Triangulation distance measurement

The principle of triangulation distance measurement is shown in Figure 5-8. Light emitted from a light source (LED or LD) is focused by a light projection lens to strike the target object, and light reflecting from that object is input via a light receiving lens onto the PSD photosensitive surface. If we let the distance between the PSD and light source (baseline length) be B , the lens focal distance be f , and the amount of movement of the light spot from the center on the PSD be X , then the distance L to the target object is expressed as $L = 1/X \times f \times B$. This method offers a great advantage: the distance can be found regardless of the reflectance of the target object and variations in the light source power. This principle is also applied in laser displacement meters.

[Figure 5-8] Principle of triangulation distance measurement



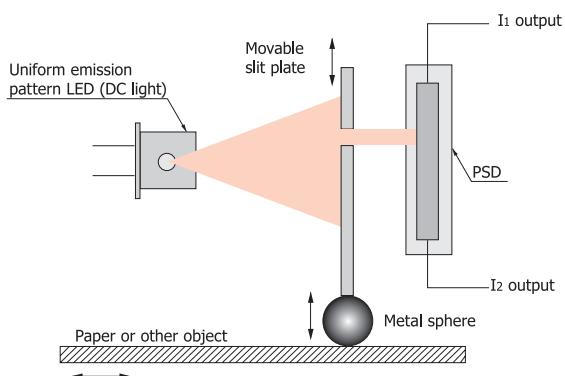
KPSDC0086EA

5-10 Direct position detection

Figure 5-9 shows the direct position detection principle. The light source (LED or LD, etc.) emits light which passes through a slit and irradiates onto the photosensitive surface of the PSD. The position where the light strikes the PSD surface shifts according to the slit movement. Calculating that position information allows finding the amount of slit displacement.

Figure 5-10 shows how this is applied to optical camera-shake correction. When a camera shake occurs due to shaky hands, the correction optical system causes a horizontal movement in the direction of the shake so that the center of the image returns to a position at the center of the film or image sensor. The PSD is utilized to detect and control movement (position information) of the slit which is built into the correction optical system.

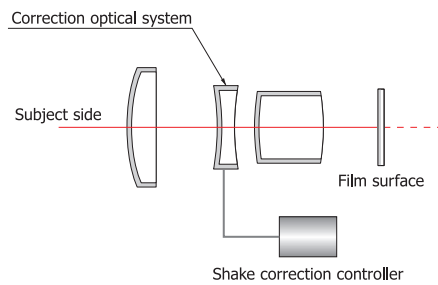
[Figure 5-9] Example of direct position detection



KPSDC0080EB

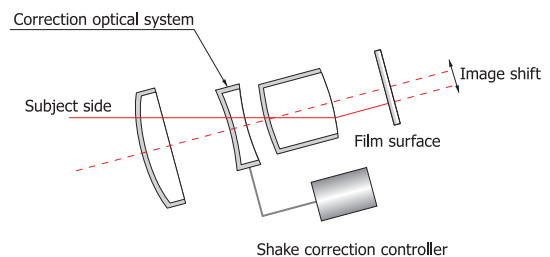
[Figure 5-10] Optical camera-shake correction

(a) State with no camera shake



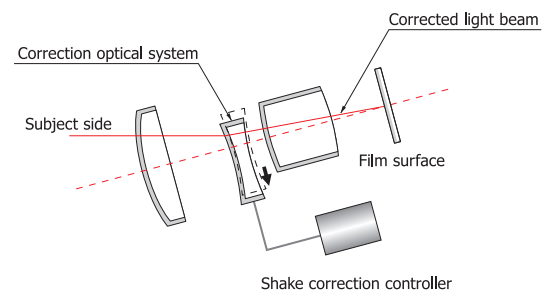
KPSDC0087EA

(b) State when camera shake occurred



KPSDC0088EA

(c) State when camera shake was corrected
(by moving the correction optical system)



KPSDC0089EA

深圳商斯达实业**专用电路与单片机部**是专业开发、设计、生产、代理、经销专用电路(ASIC)

和单片机配套产品,温度、湿度、语音、报警、计时、计步、测速、调光、游戏、新特优等专用芯片和模组;专用电路、微控制器、DSP、语音系统开发、设计、测试、仿真工具,为消费电子、通信、家电、防盗报警厂家提供专业服务。产品主要有:1、温度计电路、体温计电路、湿度计电路、时钟温湿度计电路、计时钟控电路、计步运动表电路、测速电路、调光电路、游戏电路、防盗报警电路、遥控电路、钟表电路、闪灯电路、计数电路、语音电路等专用芯片和模组,为三资企业、外贸出口企业提供完整配套服务;2、带LED闪烁电路、声效电路、玩具钢琴电路、音乐音效电路、灯串电路、风扇控制电路、计算器电路、万年历电路、汇率转换电路、玩具声光电路、遥控编解码电路、红外线遥控电路、无线遥控电路及配件、语音录放电路、圣诞灯电路、热释电控制器(人体感应)电路等专用芯片和配套模组。

更多产品请看本公司产品专用销售网站:

商斯达中国传感器科技信息网: <http://www.sensor-ic.com/>

商斯达工控安防网: <http://www.pc-ps.net/>

商斯达电子 元器件网: <http://www.sunstare.com/>

商斯达微波光电产品网: [HTTP://www.rfoe.net/](http://www.rfoe.net/)

商斯达消费电子产品网: <http://www.icasic.com/>

商斯达实业科技产品网: <http://www.sunstars.cn/>

传感器销售热线:

地址:深圳市福田区福华路福庆街鸿图大厦 1602 室

电话: 0755-83387016 83387030 83398389 83600266

传真: 0755-83376182 (0) 13902971329 MSN: SUNS8888@hotmail.com

邮编: 518033 E-mail: szss20@163.com QQ: 195847376

深圳赛格展销部: 深圳华强北路赛格电子市场 2583 号 电话: 0755-83665529 25059422

技术支持: 0755-83394033 13501568376

欢迎索取免费详细资料、设计指南和光盘;产品凡多,未能尽录,欢迎来电查询。

北京分公司: 北京海淀区知春路 132 号中发电子大厦 3097 号

TEL: 010-81159046 82615020 13501189838 FAX: 010-62543996

上海分公司: 上海市北京东路 668 号上海赛格电子市场 2B35 号

TEL: 021-28311762 56703037 13701955389 FAX: 021-56703037

西安分公司: 西安高新开发区 20 所(中国电子科技集团导航技术研究所)

西安劳动南路 88 号电子商城二楼 D23 号

TEL: 029-81022619 13072977981 FAX: 029-88789382